A Novel and Comprehensive Artifact Reduction Strategy for EMG Collected During fMRI at 3 Tesla

A Thesis

Submitted to the Faculty

of

Drexel University

by

Jaimie B Dougherty

in partial fulfillment of the

requirements for the degree

of

Doctor of Philosophy

June 2010

Dedications

First and foremost I dedicate this thesis to my family. To my husband Ryan for his continuous support and encouragement despite listening to me talk about things he has no interest in for 5 years now. For his willingness to help around the house, his suggestions of music that assist programming and his ability to always make me smile and know that I can do this, he has my deepest thanks, appreciation, and love. To my parents for always believing in me and teaching me to demand my absolute best from myself. To my brother, who listens and gives constant support and strength. To my sister-in-law for reading all these chapters and making me use commas. And to Bear and Nemesis, who know that a tail wag encourages and walks give room for thought.

Acknowledgements

It is a pleasure to thank those who made this thesis possible. I owe my deepest gratitude to my advisers Dr. Karen Moxon and Dr. Feroze Mohamed who supported me with advice, feedback, discussion, and a great deal of patience. Both opened their doors and helped me develop my ideas and thinking to the level they have reached today.

I am grateful to Dr. Scot Faro for his support of this research. I also would like to show my gratitude to Chris Conklin for giving his time to assist in data acquisition and for teaching me SPM8.

I would like to acknowledge Shriners Hospital for Children as well as Temple University Hospital for their support of this research and the use of equipment and facilities.

Finally I am indebted to all my colleagues and friends who volunteered their time as subjects and to my friends and family for their unending support and encouragement.

Table of Contents

List of Tables

List of Figures

Abstract

A Novel and Comprehensive Artifact Reduction
Strategy for EMG Collected During fMRI at 3 Tesla
Jaimie B Dougherty

Functional MRI (fMRI) studies utilizing simultaneous and reliable electromyography (EMG) data can provide valuable functional output parameters to enhance image analysis and improve the study of brain function. Although strategies have been developed to reduce the noise in EMG signals collected during fMRI, few studies report rigorous validation or examine techniques in atypical EMG. In this work, a novel wavelet based artifact reduction tool is described. Stringent validation of the technique is performed in typical and fatigued EMG signals acquired from 10 typically developed subjects while collecting fMRI images at 3 Tesla. In the novel strategy, the signal is band-passed for the EMG spectrum. Periods of muscle activity are identified with a double threshold strategy based on amplitude of the signal. The stationary wavelet transform is employed using an 8 level analysis and thresholds optimized to remove artifact with minimal impact on EMG parameters. The artifact corrected EMG is analyzed traditionally for median frequency, power, and amplitude by root mean square. The technique removes visible artifact from the EMG in typical and fatigued conditions, amplitude was dampened with artifact correction and median frequency was not impacted by artifact correction. Post artifact correction, fatigued EMG was distinct from the unfatigued EMG, showing a significant decrease in median frequency ranging 3 to 10 Hz. These results demonstrate wavelet denoising as a viable artifact reduction tool for use with EMG collected during

fMRI data acquisition. The work presents a method for tracking and identifying changes in muscle activity during image acquisition for fMRI studies.

Chapter 1: Overview

The ability to simultaneously collect electromyography (EMG) data during fMRI is highly desirable. EMG provides a quantitative assessment of functional output during motor tasks and can be used as a covariate to account for variance in functional images that corresponds to muscle activity, refining image results. The ability to detect changes in muscle activity in the MR environment has enormous impact on neuroimaging. With the ability to witness changes in muscle activity as well as cortical activity, relationships between muscle activity and cortical activity can be better defined, progress can be tracked and treatments assessed more accurately.

Despite the advantages of combining EMG and fMRI, a significant obstacle is that the oscillating magnetic fields in fMRI create considerable artifact in EMG recordings. Many strategies have been developed for reducing artifact in EMG collected during fMRI. However even the most commonly used technique imposes certain limitations on image acquisition. No assessment of any technique has included multiple conditions to identify the range of function for a methodology. Similarly, no study has been made of the ability to distinguish between muscular conditions in the MR environment. An artifact reduction strategy for use with EMG collected during fMRI that can retain and detect changes in muscle activity is needed. This technique must be fully explored to understand what impact reducing fMRI artifact has on the quality of the EMG signal.

1.1 Specific Aims

Aim 1: Develop a novel wavelet based artifact reduction tool for use with EMG collected simultaneously with fMRI

Objective 1.1: *Artifact reduction strategy must remove most visible artifact from EMG*

Objective 1.2: *Artifact reduction strategy must require no interpolation*

Aim 1 utilizes wavelet techniques to remove fMRI artifact from EMG. The development of this technique is focused on removing fMRI artifact with a methodology that places no constraints upon image acquisition.

Aim2: Assess the robustness of the wavelet denoising algorithm in reducing artifact in EMG collected during fMRI

Hypothesis 2.1: *Wavelet denoising of EMG collected during fMRI will result in EMG that is not significantly different from EMG collected without MR scanning. The following signal characteristics will be assessed: filtered signal, amplitude by root mean square calculation, and total power.*

Hypothesis 2.2: *Wavelet denoising of EMG collected during fMRI will result in a shift in the spectral parameter and median frequency when compared to EMG collected without scanning*

Aim 2 focuses on the validation of the methodology developed in Aim 1. The quality of EMG post artifact correction will be assessed based on traditional EMG parameters. EMG collected without scanning and EMG collected with scanning post artifact correction will be compared to validate the methodology in Aim 1 for use with EMG.

Aim 3: Asses the validity of wavelet denoising for EMG with atypical characteristics

Hypothesis 3.1: *Wavelet denoising of EMG collected during fatigued contractions during fMRI, will result in EMG that that is not significantly different from non scanning fatigued contractions EMG in raw signal vs. post processed signal, amplitude by root mean square calculation, and total power.*

Hypothesis 3.2: *Post processing, EMG collected during fMRI will show distinct changes in frequency parameters corresponding to fatigue.*

Aim 3 is the validation of artifact reduction method in atypical EMG will use the same methods and criteria as in typical EMG to demonstrate the robustness of this method.

Aim 4: Asses the effects of EMG parameters as regressors in the analysis of motor fatigue on cortical activation during voluntary ankle movements

Hypothesis 4.1: *Cortical activations, as assessed by fMRI, associated with non-fatigued ankle movements will be significantly different from cortical activations associated with fatigued ankle movements when analyzed with EMG spectral parameters as regressors.*

Aim 4 verifies the quality of functional images and explores the inclusion of EMG parameters in image analysis as random effect variables.

Chapter 2: Review of Literature

2.1 Electromyography

Electromyography (EMG) is a common tool used to observe muscle activity in medicine and research. This non-invasive and relatively inexpensive technique can provide considerable quantitative information about muscle activation patterns. As an action potential propagates and depolarizes the postsynaptic membrane of a muscle fiber, an electromagnetic field is generated around the muscle fibers. An electrode within this field can detect changes in electrical activity in muscles (Basmajian and De Luca 1985). The signal characteristics for surface EMG, measured from the skin over the bulk of a muscle, include a dynamic range from 50μV to 5 mV and the frequency content is approximately 2-500Hz though the dominant energy is in the 50 to 150Hz range (Bronzino 2006).

The most common detection tools and strategies for surface EMG recording are the use of Silver/Silver Chloride electrodes, the use of a bipolar recording configuration, and an inter electrode distance (IED) between the bipolar electrodes that ranges from 10 to 40 mm (Hermens et al. 2000). The bipolar recording configuration for use in surface EMG is the placement of electrodes at two distinct locations on a muscle, defined by the IED, so that the differential output of the amplifier highlights muscle activity with a reduction in common background noise (Turker 1993), particularly important in an environment with additional noise sources. A bipolar configuration parallel with the muscle fibers, as is most common, produces a signal that has a biphasic shape with amplitude varying randomly above and below zero (Basmajian and De Luca 1985). This signal is rectified

either by eliminating negative values or by inverting negative values to obtain a useful signal and normalized by the maximum amplitude of the maximum voluntary contraction (Hermens et al. 2000; Malek et al. 2006). Consistent IED within a study is essential since this distance can influence the spectral properties of EMG (Elfving et al. 2002) and two monopolar electrodes arranged in bipolar configuration are vulnerable to variable IED as the recording surfaces are not fixed together. Because of the variability in EMG recording techniques, clearly stating the procedures and materials used is vital (Anonymous 1997).

Traditionally, analysis of the EMG signal characteristics have been limited to either signal amplitude, onset and offset of muscle activity, estimations of level of activity, or mean and median frequency to observe frequency shift (Basmajian and De Luca 1985; Soderberg and Knutson 2000). Motor fatigue is one condition in which EMG parameters have been shown to change consistently. Fatigued EMG can be used extensively to provide information that correlates with physiological changes. Fatigued contractions show decreases in mean power frequency from 50-57% (Fuglevand et al. 1993), believed to reflect propagation velocity of the action potentials changing (De Luca 1984). Although force can be maintained at sub-maximal efforts, amplitude measurements of EMG increase during fatigue (Soderberg and Knutson 2000). At maximal levels of force, EMG amplitude drops considerably with a 60 second contraction, with the drop varying by muscle (Bigland-Ritchie et al. 1983). The parameters used to analyze EMG differ considerably and consistently when comparing normal and fatigued EMG, so fatigued EMG may be considered a condition that is different from typical EMG. Recent

guidelines for the use recommended the use of median frequency as a fatigue index and indicate that muscles contraction should be at a constant force in fatigue analysis (De Luca 1997).

2.2 Wavelet Analysis

Wavelet analysis has gained popularity in recent years for the analysis of signals with different features in the time and frequency domains. Wavelet analysis is based on translations and dilations of a single function, known as a mother wavelet, given generically as

$$\Psi_{a,b}(t) = \frac{1}{\sqrt{a}} \Psi\left(\frac{t-b}{a} \right), \quad a,b \in R, a \neq 0$$

where *a* is the scaling factor and *b* is the translation parameter (Debnath 2002). A scale between 0 and 1 results in a compression of the wavelet that corresponds to high frequencies, while a scale greater than 1 results in an elongated wavelet that corresponds to low frequencies. High scales, corresponding to low frequencies, are assessed with long time windows to have improved frequency resolution, while small scales, corresponding to high frequencies, are assessed with shorter time windows and also have appropriate temporal resolution (Debnath 2002). This aspect of wavelet analysis, in which the window varies with the scale, provides a time-frequency distribution that has both good temporal and frequency resolution. Coefficients are found for each scale that correlate the signal in each time interval with the scaled wavelet. The coefficients describe the content of the signal within the frequency band of that scale. By combining

the information from each scale, a time-frequency distribution is created showing the frequency content of the signal in each time interval (Graps 1995).

One application of the wavelet transform is wavelet denoising. In wavelet denoising the signal is deconstructed into coefficients as described above. Once the signal is deconstructed into the scales and their coefficients, thresholds are set. The thresholds for each scale may be set independently to filter the frequency ranges differently (Graps 1995). Thresholds may be hard or soft. Hard thresholds use the equation given by

$$x \text{ if } |x| > t, \text{ and is 0 if } |x| \leq t$$

where t is the threshold. This technique maintains edges well but is considered crude. Soft thresholds set coefficients that do not meet the threshold to zero and shrink other coefficients to zero by the equation

$$\text{sign}(x)(|x| - t) \text{ if } |x| > t \text{ and is 0 if } |x| \leq t.$$

This is known as wavelet shrinkage and does not create discontinuities. Soft thresholding has been demonstrated as both smooth and a good estimator in denoising (Donoho 1995). After thresholding, the signal is reconstructed. Flexibility is inherent in wavelet denoising because thresholds can be set individually for each level. Additionally, intervals can be created with thresholds specific to each interval. This feature of wavelet denoising is essential because thresholds can change with changes in the signal content. Thresholds that vary by intervals and signal content optimally remove artifact from signals. Wavelet denoising is an inherently flexible artifact removal tool that can be optimized to many applications. The flexibility and variability of wavelet denoising techniques leads to a real need to document the methods used very thoroughly.

2.3 Functional Magnetic Resonance Imaging

In all types of magnetic resonance imaging (MRI), a magnetic field is used to differentiate structures in the body, creating images of biological tissues. A static magnetic field aligns atomic nuclei with the field in high and low energy states. An oscillating magnetic field transfers energy into the system, causing many low energy state nuclei to become energized and enter a high energy state. When the oscillating magnetic field is removed, most nuclei return to the low energy state and emit photons, which are recorded by an MRI scanner as the raw MR signal. The relaxation back to a low energy state is dependent on nuclei properties, and MRI images are constructed based on the differences in properties between tissues and scanning parameters (Huettel et al. 2004).

Functional magnetic resonance imaging is focused on the workings of the brain instead of structures. That is, while MRI results are unchanging images of brain structures, fMRI results show changes in brain activity. To observe changes in brain activity, hemoglobin and blood flow can be tracked. Hemoglobin is diamagnetic when oxygenated and paramagnetic when deoxygenated. Consequently, changes in the oxygenation of hemoglobin change the relaxation properties of the blood so fMRI can be used to differentiate between active and non-active cortical regions (Toma and Nakai 2002). Regions of the brain that are active require greater amounts of oxygen and increased blood flow, so increased amounts of oxygenated blood in a particular region of the cortex implies the activation of that region. In this way, hemodynamics relate to cortical activity, though the exact relationship is still being explored (Arthurs and Boniface 2002; Dickerson 2007; Matthews et al. 2006). These changes are referred to as blood-oxygen

level dependent (BOLD) changes. BOLD imaging is useful in cortical mapping because it demonstrates what region of the brain is active during specific activity. The hemodynamic response is not instantaneous, so changes in blood oxygenation are witnessed over the period of a few seconds.

With BOLD imaging, fMRI is useful in determining the region of activity in the brain during a task and in quantifying brain activity. Analysis of cortical activation can include the area of activation, the extent of activations, or can follow the time course of hemodynamic changes. Increased activation areas are likely indicative of more cortical neurons becoming active while higher signal intensity is likely associated with a higher discharge rate for neurons (Toma and Nakai 2002). Both area of activation and extent of activation are commonly used in fMRI research as they are fairly well understood, reliable, quantitative measures. It is important to understand that cortical activation maps are the result of T-tests that compare the functional images when active to the functional images during rest, so the activation map resulting is really the regions that have changed their activation.

In all fMRI analysis, regressors may be included to improve the analysis. Regressors are variables used to explain variance in data sets. In fMRI analysis, regressors describe important information that changes between subjects or data sets. Regressors can be as simple as subject age or if the subject is a smoker, or can describe something that varies with a task, such as head movement (Johnstone et al. 2006), the number of movements in a motor task, or information that describes specific muscle activity, like EMG. When

analyzing a group of subjects or data sets, regressors can account for variation in the data set and improve the final results of the study.

In fMRI, a block design allows for easy repetitions of a motor task, which is helpful for both the images and EMG signals. In all studies, the more repetitions that can be included, the better the results of the study generally are, since in the analysis of a block design task, each of the blocks is averaged with others of the same state. These strategies are one reason that fMRI provides very accurate spatial information about where cortical activations take place. Functional images give quantitative information concerning area and extent of activation, which is used in a variety of applications including understanding more about motor control.

2.4 Combined EMG and fMRI

The ability to simultaneously collect EMG with fMRI is highly desired. By introducing the functional output of a motor task, the EMG, into the analysis of fMRI images as regressors, cortical activations can be refined to account for variations in task performance. The inclusion of temporal EMG data can enhance studies by providing improved information about when muscle activity is occurring with respect to hemodynamic changes. However, the challenges associated with combining these modalities are not minor.

The strong magnetic fields used in magnetic resonance imaging introduce constraints in patient population. For example, patients with ferrous materials or wires in their bodies

cannot enter the MRI environment. Similarly, the materials used for recording EMG during fMRI must be nonferrous (Laufs et al. 2008). Ag/AgCl electrodes are the most common electrode type used inside the MRI environment (Gonçalves et al. 2007; Allen et al. 1998; Mantini et al. 2007). Radiotranslucent carbon-fiber leads that connect electrodes to the amplifier and system are often preferred for both safety and reduced impact on the quality of images (Negishi et al. 2007)(Goldman et al. 2000). Amplifiers may either be MRI compatible or, as in many studies, the leads may be extended outside of the MRI environment so that traditional amplifiers may be used. Hardware components must be carefully selected and screened just as all patients are screened before having an MRI.

In addition to careful selection of materials, several precautions may be taken to further ensure patient safety. The oscillating magnetic field can induce current in wires or in the human body if loops are created. Consequently, patients are positioned with no arms or legs crossing, and leads are placed carefully and secured to avoid crossings (Gonçalves et al. 2007; Negishi et al. 2007; Goldman et al. 2000; van Rootselaar et al. 2007a; van Rootselaar et al. 2007b; van Duinen et al. 2005). Minimizing conductive gel by using small electrodes is another simple step that may be taken to reduce the conductive material in the MRI environment (Laufs et al. 2008). MRI has been shown to have no negative impact on the human body, and by carefully selecting MRI compatible materials and following several simple steps in protocol, EMG may be collected in this environment without endangering the patient.

Even when using MRI compatible materials, the magnetic fields present during fMRI results in considerable artifact in EMG recordings. The static magnetic field that aligns atomic nuclei introduces artifact that largely obscures the baseline. This artifact is present at harmonics of 49Hz. This artifact can be effectively removed by twisting the pair of leads for bipolar recordings (Negishi et al. 2007).

As the source of the oscillating magnetic field, radiofrequency coils introduce energy into the system and then record energy emitted from atomic nuclei returning to low energy states and are the source of a second type of noise, gradient artifact. This artifact occurs with the oscillations of the magnetic field so the timing of this artifact is dependent on the imaging parameter echo time, which is the time between energy entering the system and when the energy emitted is recorded. The gradient artifact is many times larger in amplitude than EMG recordings and has harmonics throughout the frequency range of EMG (Allen et al. 2000). The amplitude of the gradient artifact is time varying, further making the removal of this artifact complicated. Many approaches have been taken to resolve the problem of gradient artifact to obtain useable EMG during fMRI.

In early studies combining electrophysiological signals and fMRI, researchers collected EMG simultaneously with fMRI, but only EMG collected between scanning intervals was analyzed (Spiegelhalder et al. 2008; Liu et al. 2000; Dai et al. 2001; Liu et al. 2002). Although these techniques did not remove or even reduce fMRI artifact from EMG, these studies did improve understanding about the relationship between muscle activity and

cortical activity by showing both force and EMG activity as directly proportional to fMRI signal amplitude in the entire brain and in several motor areas (Dai et al. 2001).

The first group to effectively remove fMRI artifact from an electrophysiological signal used an average artifact subtraction algorithm to remove fMRI artifact from EEG recordings. This strategy has come to be known as the Allen Method. Pulses from the scanner were used to flood the amplifier to mark in time when scanning began. A sinc function interpolated EEG data during the pulse, synchronizing the epochs to be averaged. A minimum of 5 epochs were averaged together. Another sinc function was performed to synchronize the EEG with the average artifact prior to subtraction. Post subtraction, EEG data was then smoothed and an adaptive noise cancellation adaptive filter was applied. The Allen method was validated by calculating the percent difference between EEG collected without scanning and artifact-corrected EEG collected during scanning, reporting a range from a 10-18% difference in amplitude. No spectral analysis of the artifact-corrected EEG was performed (Allen et al. 2000). The Allen method removed most artifact when inspected visually though it can be argued that because of the time-varying amplitude of fMRI artifact, an average subtraction method will never perfectly remove the artifact (Laufs et al. 2008). Regardless, the Allen Method remains the most common artifact removal strategy as it is available in commercial software.

The Allen Method has been applied to EMG collected during fMRI as well as to EEG. Minor modifications were made to the strategy, modifying the high and low pass filter to be appropriate for the EMG signal range and to remove low frequency movement

artifacts. In this validation of the Allen Method for EMG, two strategies were used. An ANOVA for repeated measurements was used to compare normal EMG with artifact-correct EMG, and a strategy for assessing clinical measurements described by Bland and Altman was used. The validation method used a Bland-Altman plot, a graphical validation that compared both normal EMG and artifact corrected EMG as well as the average differences in the measurements and showed that the variability in the corrected EMG was less than the normal physiological variability, supporting this artifact reduction strategy. This study utilized the most extensive validation of an artifact reduction strategy, comparing artifact corrected EMG with normal EMG. This method demonstrated a high correlation between artifact corrected and normal EMG, no significant differences were found in the total power, and no significant differences were found in the median power frequency (van Duinen et al. 2005). However, despite utilizing the Allen method, differences in amplitude between corrected and normal EMG were not analyzed as in the original Allen work and no atypical conditions were tested. Lacking this analysis, the full effects of the artifact correction on EMG are still not documented. Though this study performs the most extensive validation of their work, several components remain missing.

In an approach that varies from artifact subtraction, principal component analysis and independent component analysis have been used to remove fMRI artifact from EMG. In this strategy, several repetitions of the signal were combined and decomposed into principal components, or the identifying features of the data. At this stage for the ICA analysis, ICA was used with the principal components as the starting input. Both

processing strategies evaluated the components, discarded those identified as noise, and reconstructed the signal. The artifact reduction was evaluated by the contrast ratio, defined as the average amplitude of the EMG signal during movement over the average amplitude during rest (MacIntosh et al. 2007). The use of contrast ratio for validation was useful in some respects. If the focus of the EMG/fMRI study is just timing, this is a good strategy. However, the question of how the artifact reduced EMG compares with typical EMG is never addressed. For the purposes of differentiation between active and rest periods, this method is effective, but if properties of the EMG are the purpose for recording EMG, the principle component or independent component analysis technique presented here is not adequate.

Many studies focus on the best ways to remove artifact from EMG collected during fMRI and there is little dispute over the value of collecting EMG during fMRI. However, few studies have actually explored the use of EMG in the analysis of the functional images. In a validation of the use of EMG regressors in the analysis of functional images, EMG amplitude was used as a single regressor of interest during analysis and the activation maps were compared with activation maps found with traditional block design analysis. Cortical activation maps using EMG amplitude as a single regressor were very similar to conventional block design analysis maps, but were better refined. The same basic regions were active, but the EMG amplitude maps had fewer active voxels. A similar experiment compared activation maps of a task with both fast and slow movements. In this comparison, mean EMG power was assessed and adjusted by active and inactive blocks to give a residual EMG that reflects changes in EMG activity. Similar to the

EMG amplitude as a regressor, residual EMG maps had similar activation maps to traditional block design analysis, but again, fewer voxels were active (van Rootselaar et al. 2007b). This study demonstrated that EMG parameters may effectively be used in functional image analysis though the study seems incomplete in that it never combined EMG activity with traditional block design analysis.

In a study of force modulation and motor fatigue, an EMG parameter that reflected changes in EMG activity was used as a regressor in the fMRI analysis so that regions of the brain with activity that correlated with EMG activity were identified (van Duinen et al. 2007). This analysis showed changes in central activations that related to peripheral output, but failed to compare results obtained including EMG parameters as regressors in comparison to results without EMG parameters as regressors. Both van Rootselaar et al and van Duinen et al. studies have shown that EMG may be used as a regressor when analyzing functional images, but have not completed an analysis of the value of including EMG parameters other than amplitude with traditional block design analysis.

The inherent difficulty in combined EMG or EEG and fMRI is the lack of stringent validation. There is no agreed upon gold standard for artifact reduction techniques in this field, leading to no consistency and in the validation methods reported. Even studies that assess the differences in artifact corrected signals in comparison to signals collected without the noise source are incomplete. No known studies explore the full effects of artifact removal on the signal in question. Spectral analysis is very rare in the literature, and when it does occur, other validation components are lacking. Despite, or perhaps

because of, the lack of a gold standard and stringent validation when combining EMG or EEG with fMRI, many techniques have been used and published that lack basic information about the effects artifact reduction has on signals. Similarly, studies that utilize EMG parameters in their analysis fail to fully explore the influence of including functional output information. These gaps must be remedied for studies that use both EMG and fMRI to be truly valid and complete. Without answering questions about the quality of the EMG obtained and the influence of EMG as an included regressor, it is difficult to evaluate results.

2.5 Motor Fatigue

Motor fatigue has been explored a great deal because it not only links many neuromuscular conditions as a limiting factor of activity and quality of life, but also because most athletic injuries occur during periods of fatigue. Although motor fatigue has been studied extensively at the muscle and even spinal level, understanding of cortical activity during and after motor fatigue remains limited. Functional activations associated with motor fatigue may lead to improved understanding of control mechanisms and motor drive.

Benwell et al. explored how functional activations change after fatiguing exercise. This study used visual cues to signal the subject to squeeze a spring-loaded handgrip. The fatiguing exercise consisted of 10 minutes of three seconds of 30% of maximal force followed by two seconds of rest. Functional scans were taken prior to fatiguing exercise as well as immediately after, and then another during fatigue recovery. This study found

decreases in cortical activation in the primary sensorimotor cortex, the supplementary motor cortex, the cerebellum, and the primary visual cortex. The drop in activations in motor areas post fatigue is well documented in several studies though this particular study did not explore the time course of the hemodynamic response to fatigue, only observed changes post fatigue and during recovery. This study also failed to quantify the fatigue beyond showing the drop in force at the end of the fatiguing exercise. The inclusion of reaction time to visual cues was intended to provide information about attention, though it allows for question about mental fatigue and the true cause of the decreased activation in the visual cortex (Benwell et al. 2006). This study was not optimally designed since it did not include functional scans during the fatiguing exercise, but it does provide clear documentation about the patterns of activation post fatigue.

One difficulty in studying motor fatigue is that fatigue is a very qualitative condition. Assessments of fatigue are often very subjective, so quantifying fatigue has long been desired in motor fatigue studies. Years of research have led to an understanding of how muscle activity changes during fatigue conditions, so EMG amplitude and spectral parameters, mean frequency and median frequency, may be used to show fatigue. During submaximal sustained contractions, EMG amplitude increases to maintain force levels. Under all fatigue conditions, both mean frequency and median frequency decrease significantly (Bigland-Ritchie et al. 1983).

To explore of how cortical activations change during fatigue conditions, EMG, force data, and fMRI were collected simultaneously using 2 minute contractions at maximal

contraction and 5% of maximal effort. Continuous EMG was not analyzed, only EMG collected between scans. During 2 minute long maximum voluntary contractions, total cortical activation first increased and then decreased. The EMG activity decreased nonlinearly over the 2 minute contraction (Liu et al. 2002). These results provided information about the course of functional activations during fatigue, showing that the decrease in activations associated with fatigue is not immediate. The time course of fatigue was not fully addressed as EMG data was not combined with functional activations.

In a similar study, sustained and intermittent submaximal contractions were analyzed during fatigue. This analysis focused on exploring how functional activations vary with different types of fatiguing exercise. EMG and force data were collected simultaneously during imaging, but only EMG from between scans was analyzed. During submaximal sustained contractions, force remained constant while EMG amplitude increased and then hit a plateau. The overall cortical activations increased over most of the task though a plateau was reached in the last third of the 3 minute task. It was concluded that brain increased its output to continue to stimulate the muscle sufficiently to maintain the steady force (Liu et al. 2003). The analysis of active regions of the brain over the course of the task was beneficial in exploring the time course of the relationship between functional output and the areas of the brain. However, this study did not analyze continuous EMG and include it in their analysis, which would have been a good addition to the study.

In another study by Liu et al., the fatigue exercise performed was an intermittent maximum voluntary contraction. Over the course of these short contractions and rests, EMG and force decline approximately 40% while most motor areas did not significantly change their activations. Only the primary sensorimotor cortex showed a decline in activation. This study demonstrated that the type of task, while not necessarily impacting the output at the local level of the muscle, does influence the central mechanisms. The importance of clearly documenting and reporting the tasks performed is very clear. However, this study did not fully utilize their EMG and force data. Force data, EMG, and fMRI activations were combined for a statistical analysis, but only EMG from between scans was used, and neither EMG nor force were included in the analysis of the functional images (Liu et al. 2005). Although research in which EMG and fMRI are combined has increased dramatically in the past few years, few studies are really capitalizing on the additional information collected during functional scans.

Continuous EMG has been collected and analyzed in motor fatigue studies though the EMG signal is not often used extensively in the analysis. In a study that explored functional activity during sustained maximal contractions, EMG was studied in a statistical analysis though the EMG results were not directly linked to the functional activations or hemodynamic response timing. Mean frequency was assessed to confirm fatigue from the beginning to end of sustained contractions. This study showed increases in motor areas during the motor task and decreases in the voluntary activation of the muscle. These results suggested although that the cortical activity was increased in motor

areas, the increased activation could not overcome fatigued-related changes in voluntary drive of muscle activity (Post et al. 2008).

In the first work to incorporate EMG as a regressor in a motor task in an fMRI study, a scaled EMG was first found. Scaled EMG was based on the mean amplitude summed from several muscles and normalized by the standard deviation. This EMG parameter was shifted 6 second to account for the slow hemodynamic response, and then was included as a regressor in two tests. Scaled EMG was used to identify regions associated with force modulation as well as modulation of motor drive in fatigue. This study utilized the qualitative information about muscle output to improve analysis. By using scaled EMG as a regressor in these analyses, the resulting activation maps reflected activations that correlated with EMG activity and did not necessarily correspond to more or less activity overall (van Duinen et al. 2007). Although this work incorporated EMG into the analysis of functional images, several steps remain to be taken. As in other works, the analysis was not compared with and without the use of EMG as a regressor. This study did show the changes in EMG with time for different levels of contractions, but it would have been beneficial to show these changes with the hemodynamic response.

Chapter 3: Develop a novel wavelet based artifact reduction tool for use with EMG collected simultaneously with fMRI (Aim 1)

3.1 Introduction

Although several strategies have been developed to reduce artifact in EMG collected during fMRI, no current technique provides the user with flexibility, validation, versatility, and excellent function. Average artifact reduction strategies require a pulse to be emitted at the beginning of each scanning sequence to align artifact in time and have not been evaluated for versatility (van Duinen et al. 2005; Allen et al. 2000). Artifact reduction strategies based in independent component analysis or principle component analysis require several repetitions of EMG to be combined, requiring several repetitions of fMRI acquisition for a single set of EMG data (MacIntosh et al. 2007). Methods which do not include the entire EMG, but only analyze EMG collected between scans do not require multiple repetitions, but also do not reduce artifact in the signal and only use a fraction of the EMG data.

The first aim in this research was the development of a flexible artifact reduction strategy for removing fMRI artifact from EMG signals. Wavelet denoising was selected because of the inherent flexibility in wavelet analysis. Additionally, wavelet denoising is well suited to fMRI motor studies because motor studies include the repeated performance of some motor task. This repetition results in EMG with a sequence of activity and rest for each muscle being evaluated as the muscle must relax for the motor task to be repeated. Intervals of activity and rest have different signal content, and this remains true when artifact is present, allowing for wavelet denoising to be optimized for the signal in each

interval. This work is the first known instance of wavelet analysis for artifact reduction of EMG in the MR environment.

3.2 Methods

Subjects

For this work, 10 right-dominant adult subjects with no known neuromuscular abnormalities were recruited from a sample of convenience made up of associates through Drexel, Shriners, Temple, and friendships. Subjects recruited were between the ages 18 and 35 (mean 27 ±2.6) and were recruited regardless of gender. Subjects were required to have visioperceptual skills and cognitive/communication skills sufficient to follow commands and to attend to tasks associated with data collection. Exclusion criteria included metallic or electrical implants including braces, history of claustrophobia or seizures, pregnancy, and subjects unable to remain still for the duration of the exam. All the studies conducted in this work were approved by both Temple University and Drexel University Institutional Review Boards.

Experimental Protocol

Before the experiment started, subjects practiced the motor task. The task consisted of a series of rests and ankle movements. The experimental protocol utilized a basic block design with 4 repetitions. Alternating 30 second blocks of rest and activity took place for a total of 4 minutes. The motor task consisted of strong right ankle movements through the active range of motion at a self-selected pace. Verbal instructions to rest or begin movement were provided by the fMRI technician through headphones. The head was

immobilized using foam pads and tape. The ankle was supported by a pillow to enable a full range of motion without moving the leg. Prior to scanning, the subject practiced the task to confirm EMG setup and ensure the subject was comfortable with the instructions before beginning data collection and introducing fMRI artifact into the EMG. Three maximal voluntary contractions (MVCs) were performed, lasting approximately two seconds each with up to 20 seconds of rest between them.

fMRI Measurements

A Magnetom Verio 3Tesla scanner with TIM technology was used to obtain images (45mT/m, rapid switching gradients). Scanning began by acquiring high-resolution T1-weighted imaging sequences in the axial plane to locate the positions for in-plane structural images. Imaging parameters were: matrix size = 256*256; TR (repetition time) = 1600 ms; TE (echo time) = 2.51 ms; FOV (field-of-view) = 240 mm; NEX (number of excitations) = 1; and slice thickness = 0.9mm. Contiguous (no gap) axial images were acquired to cover the entire brain.

Functional images were obtained with echo planar free induction decay (EPI-FID, T2* weighted) sequences in the same plane as the structural images in an interleaved order. The functional imaging parameters were a 64*64 matrix; FOV = 210mm; slice thickness = 5mm; TR = 3 s; and TE = 21 ms. The size of the imaging voxel was 3.28 mm x 3.28 mm x 5 mm. A 12-channel brain phased array coil was used for imaging. Each block consisted of 10 measurements covering the entire brain.

EMG Measurements

For EMG measurements, two 4mm diameter monopolar silver/silver-chloride electrodes with radio-translucent carbon fiber leads (Biopac) were placed in bipolar configuration on the anterior tibialis following Clinical SEMG Electrode Sites from NORAXON EMG & Sensor systems. An interelectrode distance of 15mm was used, chosen based on a literature review (Elfving et al. 2002) and the need to minimize the difference in location within the magnetic field while maintaining two distinct recording sites (Laufs et al. 2008). The carbon fiber pair of leads was twisted to reduce artifact, minimizing the artifact effects of the static magnetic field (Gonçalves et al. 2007). A reference electrode was placed on the knee of the same leg to minimize differences in the magnetic field between reference and recording electrodes. The leads were extended outside the MRI environment with an MRI cable/filter set from Biopac through a waveguide conduit. A custom connection to a conventional EMG system (Myomonitor III – Delsys), was created to connect all electrodes to the amplifier. The PC was equipped with EMGWorks software for controlling acquisition with a sampling rate of 1200 Hz.

EMG processing

All of the EMG data were processed in Matlab® (The Mathworks, Inc., Natick, MA). A 12^{th} order Butterworth passband filter was applied to all data. The high-pass frequency of 15Hz was chosen to remove movement artifacts. The low-pass cutoff frequency 350Hz was selected as the magnitude of frequency content in EMG above 350 is minimal while the artifact remains strong.

For EMG collected during scanning, the following process was applied to identify periods of activity and rest. EMG onset and offset points were identified by a double threshold based on amplitude changes and artifact characteristics. A window of 8.3ms was translated across the signal, finding the largest change in amplitude across the window. Windows with the maximum difference in amplitude within 0.257 mV and 1 mV were identified as on periods while those exceeding the maximal threshold were identified as artifact and those below the low threshold were identified as off periods. Thresholds were selected based on EMG characteristics when collected outside of an MRI environment to ensure proper signal characteristics with the given system. Periods identified as artifact were assigned an arbitrary off value. Since there is the possibility of false positive identification of on periods, the secondary algorithm was based upon off periods. A 83ms window was translated across the signal, identifying what fraction of points was identified as off in the window. If at least 15% of the points in the window were identified as off, the entire window was set to off. If less than 15% of the points in the window were identified as off, the window was set as on. From this double threshold, a vector of on and off points was created for each data set, identifying active and rest intervals for all EMG.

After a vector of on and off points was created, wavelet denoising was performed to eliminate artifact in the following manner. The data were deconstructed with an 8 level stationary wavelet transform (swt) using a biorthogonal wavelet (bior3.9) as the mother wavelet. The swt was selected for its improved translation invariance in comparison to

the discrete wavelet transform. The swt is advantageous in that the entire signal is retained for analysis with no downsampling.

The choice of 8 levels ensured sufficient frequency resolution at low frequencies as the dominant energy of EMG is in the 50-150Hz range (Basmajian and De Luca 1985). The mother wavelet was chosen based on similarity to EMG signals, the retention of the greatest power of the EMG signal, and on the best artifact reduction during visual inspection.

Traditional threshold strategies were not applicable for EMG with fMRI artifact. Both the fMRI artifact and EMG have similar white noise characteristics. Consequently, existing threshold strategies could not differentiate between EMG and fMRI artifact. A new threshold system was developed for periods of EMG activity, based on optimizing power retention while maintaining EMG characteristics though visual inspection was used to establish if artifact remained. Thresholds were originally based upon early data from a single subject. As data acquisition progressed, it was evident that the wide range in spectral properties from subject to subject caused the original thresholds to be inappropriate for later subjects. Thresholds were then optimized to retain median frequency parameters for the greatest number of the subject population possible. As each subject's data was introduced, the thresholds were refined. Once all subjects had been evaluated and thresholds had been developed for the group, total power and amplitude were also considered, refining thresholds further. Visual inspections as well as evaluations of median frequency, total power, and amplitude were performed at many

stages to ensure false EMG was not being created from the artifact. Empirical data for the individual as well as the group results were included in the analysis of thresholds.

Final thresholds selected for denoising the signal are shown in Table 1 as well as the frequencies that correspond with each level of decomposition. Note the overlap in frequencies between levels. This overlap allows for fine adjustments to frequency content. Level 1 was largely reduced by the band pass filter earlier applied. Remaining frequency content was filtered with a low threshold. The level 2 threshold was essential in retaining a great deal of the high-frequency content of the EMG. A slightly higher threshold allowed for the EMG to be retained while removing artifact in this band. The slightly higher threshold allowed more signal to be retained, but the threshold was chosen to balance eliminating artifact with retaining EMG. Similarly to level 2, a great deal of both EMG and artifact was present in the frequencies associated with level 3. Therefore the threshold for level three was still low, but slightly higher than level 2 at 4.5E-5. Level 4 is a more narrow band with yet more artifact present than in the previous bands. A lower threshold for this level removes this artifact while retaining most of the EMG. Level 5, has very similar characteristics to level 4 and therefore a similar threshold was applied with some fine adjustment. Level 6 was the last level that contained EMG. This level required a threshold low enough to remove the last of the artifact, but high enough to keep EMG. Level 7 ensured that the high-pass movement filter created no additional artifact at the cutoff point with the establishment of a high threshold. Level 8, the lowest frequencies of all, were entirely within the movement filter, and ensured that the filter

was in fact removing all artifact related to movement so was very high to not allow any remaining movement artifact through.

Once the on thresholds were established, thresholds for the intervals in which no EMG signal was present were found, based on the signal content including only fMRI artifact. Thresholds for the off intervals were more stringent by an order of 10 than on interval thresholds due to the presence of EMG content in on intervals. All thresholds were chosen to be soft as the dampening properties of a soft threshold better removed artifact and maintained a continuous signal.

Table 1: Optimal thresholds for the on intervals with the biorthogonal wavelet (3.9) for removing artifact from EMG collected simultaneously with fMRI

	Level							
	1	2	3	4	5	6	7	8
Frequency Range (Hz)	205-395	109-353	54-207	29-99	16-48	9-26	8-13	1-10
Threshold	1.90E-5	3.65E-5	4.50E-5	2.00E-4	2.50E-4	3.00E-4	1.00E-2	5.00E-1

Post artifact reduction, all EMG data were analyzed traditionally. Determination of EMG characteristics included calculation of the parameters amplitude by root mean square (RMS), total power, and median frequency for all subjects. Each contraction was analyzed individually. Mean amplitude, mean total power, and the average median frequency for each condition were found for each subject.

3.3 Results

In an assessment of the development of the artifact correction strategy, EMG from a representative subject is presented in Figure 1. Without scanning, EMG activity is clear with three contraction taking place within 25 seconds. EMG collected during scanning, however, is very noisy. It is difficult to identify muscle contractions and the artifact is obscuring all valuable data. The amplitude of the artifact varies but is approximately at the same level as the EMG contractions, around 0.75 to 1mV. Post artifact correction by wavelet denoising artifact has been largely reduced and muscle activity is evident with distinct contractions. No interpolation or smoothing were used.

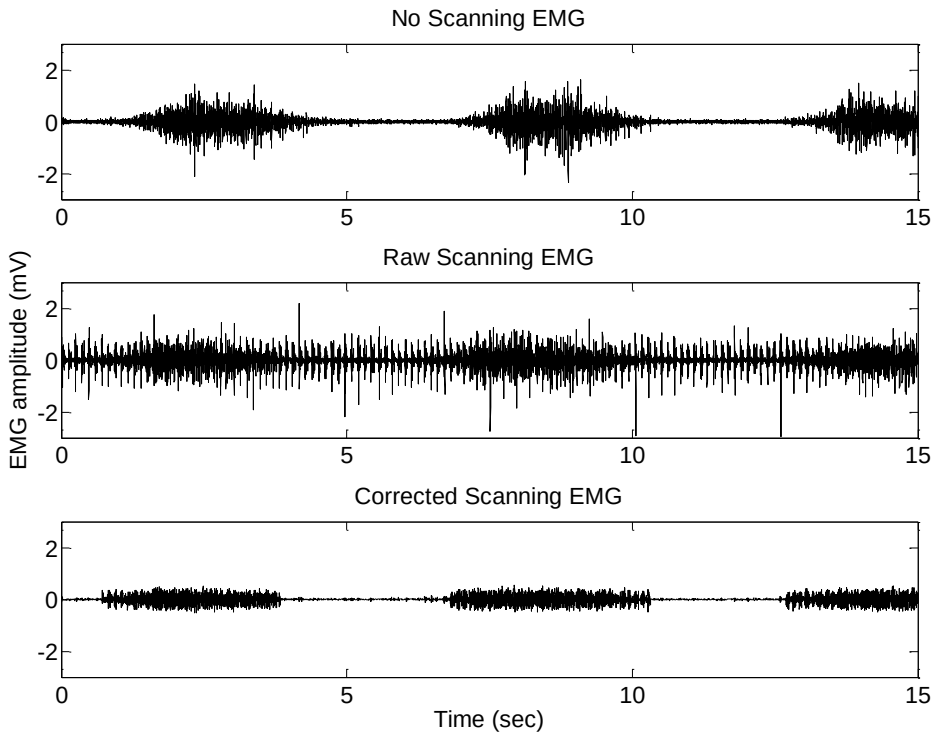

Figure 1: EMG from a representative subject in the typical condition without scanning (top), with scanning pre (middle) and post (bottom) artifact correction

Although the artifact was greatly reduced in the representative subject and the methodology used was flexible in that no specific fMRI scanning parameters were required, by looking at a second representative subject, a better understanding of the artifact and its removal can be gained. A second representative subject's data is shown in Figure 2 2. At the same scale as the previous subject, EMG is barely visible when no scanning is taking place. The amplitude for this subject was much lower than that for the first subject, a common variation between subjects. Muscle tone and activity level for this subject were also lower than the previous subject displayed. In the raw scanning data at the same scale, the artifact completely obscures the EMG. Also note that the amplitude of the artifact is greater in this subject, often in the 1-2mV range. Despite this difference in artifact amplitude, post artifact correction, the EMG for the second representative subject is very clear. The EMG is actually more visible post artifact correction than in the no scanning condition due to background noise in the room. The amplitude for the second subject remains low, but clear bursts of muscle activity can be identified with ease.

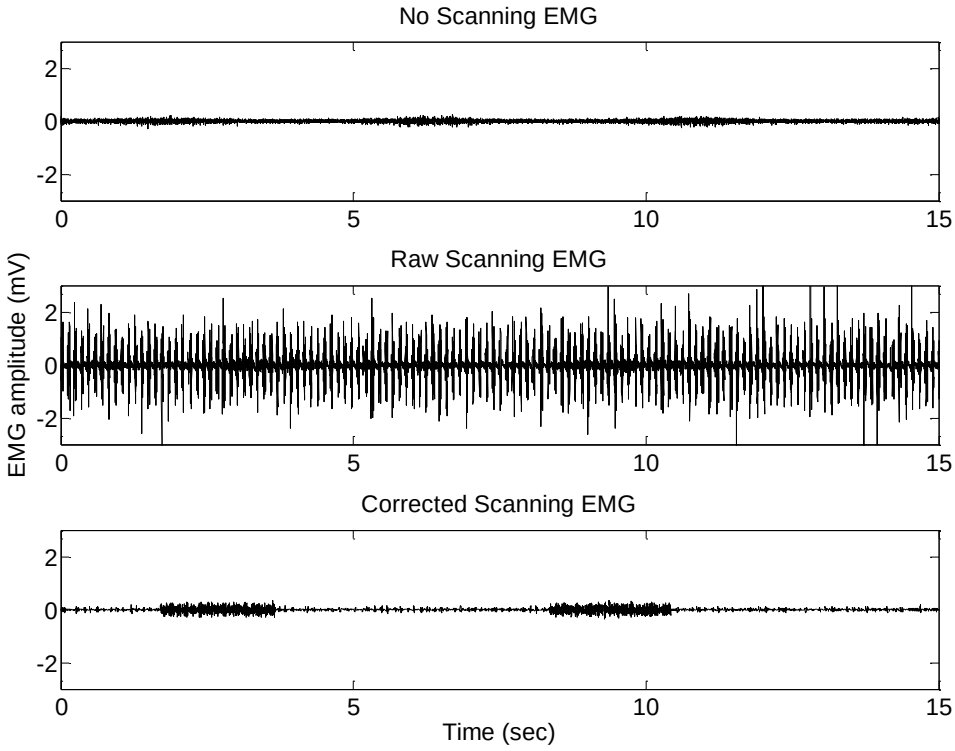

Figure 2: EMG from a second representative subject in the typical condition without scanning (top), with scanning pre (middle) and post (bottom) artifact correction

3.4 Discussion

Wavelet based artifact reduction is inherently flexible. This methodology does not depend on imaging parameters and would transition to event related fMRI studies well though block designs were used for this acquisition. The use of custom thresholds that vary by decomposition level allows for a refined artifact reduction. The creation of intervals, in this case identifying where muscle activity is present as opposed to only artifact, improves the analysis further, allowing for the nearly complete suppression of artifact while retaining EMG bursts.

Although the amplitude of the artifact ranges from subject to subject and varies throughout data collection, with the use of wavelet based artifact reduction, EMG is extracted for each subject. The differences in artifact amplitude do not influence the function of this methodology. The same thresholds used to remove artifact in the first representative subject, who had EMG with a much stronger signal and artifact with lower amplitude, were also effective for the second representative subject for whom the signal to noise ratio was very different.

EMG signals have a wide range of properties from subject to subject. Although differences in amplitude are evident here, there is also a great deal of variability in the shape of the power spectrums. It is vital that an artifact reduction strategy be able to remove artifact and retain EMG for all subjects, even those with particularly low amplitude EMG. Many patients with neuromuscular abnormalities have poor muscle tone and bulk. As a result, low amplitude EMG is often present in such cases. The second representative subject provides conditions in a typically developed subject that suggest this methodology will transition well to subjects with atypical neuromuscular development.

Preliminary work was done in a 1.5 Tesla scanner. Although in preliminary work, the thresholds were optimized for an individual subject at 1.5 Tesla the methodology was otherwise the same as presented here. Artifact was reduced well and EMG was retained with minimal impact on the quality of the signal. The transition from a 1.5 Tesla scanner in the preliminary work with an echo time of 54ms to a 3 Tesla scanner with a much short

echo time (21ms) did require the thresholds to be reevaluated and optimized for the group. However, wavelet based artifact reduction was effective in both conditions which indicates that wavelet based artifact reduction is very versatile. This versatility will allow researchers and doctors to optimize their experimental design to obtain the needed images with the assurance that the quality of EMG will not be compromised.

Current published artifact reduction techniques for EMG collected during fMRI range considerably and all impose some sort of constraints on the experimental design. Independent component analysis and principle component analysis both require many repetitions (MacIntosh et al. 2007). Multiple repetitions of EMG are combined so users cannot evaluate every individual contraction or track how EMG is changing over time, which can provide valuable information when combined with fMRI results. The Allen method, based in average artifact subtraction, is quite flexible but requires a pulse to be emitted by the scanner at the beginning of each TR which enables the average artifact waveform to be developed (van Duinen et al. 2005; Allen et al. 2000). This strategy also requires interpolation at two stages and relies heavily on smoothing after the average artifact has been subtracted from the EMG. Though the Allen method has been widely used, wavelet based artifact reduction allows for a great deal more flexibility in experimental design and does not rely on smoothing. With the elimination of smoothing, EMG amplitude can be evaluated with confidence that the end amplitude measurements are in fact entirely based on EMG and not on artifact.

Wavelet based artifact reduction is a very versatile technique that has been shown to reduce artifact in EMG signals and provide clear contractions post correction. The technique is effective and can be used with a wide range of imaging acquisition parameters. This strategy introduces a flexibility into combined EMG and fMRI that was not present previously.

Chapter 4: Assess the robustness of the wavelet denoising algorithm in reducing artifact in EMG collected during fMRI (Aim2)

4.1 Introduction

We see in Chapter 3 that the newly developed wavelet based artifact reduction strategy for EMG collected during fMRI does remove artifact. The versatility of the methodology was discussed and it was shown that artifact is removed from subjects who have very different EMG from one another. In fact, the variation in muscle tone, bulk, and overall activity level within the subject population demonstrates that the artifact reduction strategy effectively removes artifact for a wide range of subjects, indicating the versatility of the described method. The previous chapter also showed that despite large variation in the amplitude of the artifact and EMG between two subjects, the artifact was reduced effectively in both cases. But simply showing that artifact has been removed is not enough. The quality of the remaining EMG must be evaluated to validate an artifact reduction technique.

Previously published artifact reduction strategies used a wide range of methods to evaluate the quality of EMG post artifact correction. The best method for showing that the quality of the retained EMG is still of an acceptable level is to compare artifact-corrected EMG with EMG collected identically but with no scanning (Laufs et al. 2008). Parameters in the time domain such as amplitude must be evaluated as well as a direct comparison of the bursts of activity. Spectral parameters that reflect the frequency content of EMG are also of importance. The total power gives a good overall assessment

of whether the full EMG signal is being retained, and the median frequency provides information about the shape of the power spectrum.

As individuals have a wide range of EMG parameters, from amplitude to median frequency to total power, it is vital to assess the quality of the EMG retained for each subject individually. In particular, the power spectrum can vary greatly in shape between subjects, so a careful evaluation of spectral parameters is of upmost importance. For an artifact reduction strategy to be implemented successfully, the exact influence the technique will have on the quality of acquired EMG must be fully known.

4.2 Methods

Subjects, experimental protocol, fMRI measurements, and EMG measurements were the same as used in Chapter 3.

EMG Processing

EMG was processed as described in Chapter 3. Post artifact correction, bursts of EMG activity were analyzed individually for amplitude by root mean square, median frequency, and total power. This provided a distribution of each parameter for each subject in a given condition. All values for a given parameter in a condition for a subject were found and combined to increase the power of statistical analysis. Mean values and standard deviations were found for each EMG parameter. Percent differences were calculated to establish what effects were present with this artifact reduction strategy in place.

Statistics

To evaluate the hypotheses of Aim 2, several statistical analyses were performed. EMG collected with no scanning (NS EMG) and corrected scanning EMG (CS EMG) were analyzed individually for each subject in the following manner. Each contraction was analyzed for amplitude calculated by root mean square, median frequency, and total power using traditional EMG analysis techniques. To account for variation between subjects, all data sets were normalized to the individual's maximum voluntary contraction. The average amplitude, median frequency, and total power were found for each subject in each condition. Each EMG burst was analyzed and combined to produce a distribution of each parameter for each condition (no scanning, scanning) in every subject. A power analysis was performed for each subject to confirm adequate sample sizes for statistical analysis.

For Hypothesis 2.1 and 2.2, an ANOVA for repeated measures was used to compare the data sets of each subject's NS EMG and CS EMG conditions. A direct comparison of the EMG bursts was performed as well as evaluation of the amplitude, median frequency and total power. P values were found for each parameter to evaluate the quality of the EMG corrected with the proposed artifact reduction strategy. The percent change with artifact correction was also tracked for amplitude, total power, and median frequency.

4.3 Results

The number of contractions performed by each subject varied and the minimum number of contractions for analysis in all conditions for each subject is shown in Table 2.

Table 2: Minimum number of contractions for each subject used in analysis

	Minimum Sample Size
Subject 1	27
Subject 2	29
Subject 3	15
Subject 4	17
Subject 5	5
Subject 6	13
Subject 7	16
Subject 8	22
Subject 9	10

To evaluate the robustness of the artifact correction strategy, the NS EMG was compared with the CS EMG for each subject. When directly comparing the EMG bursts, no significant difference was found ($p<0.05$) in any of the subjects. Most (7/9) subjects showed no significant difference in the median frequency, as seen in Table 3. No change in median frequency exceeded 5% and no significant change in median frequency exceeded 3.59%.

Table 3: Average median frequency values and changes with artifact correction

	Median Frequency (Hz)			
	NS EMG	CS EMG	% Change	Significant at $p<0.05$
Subject 1	141.15	146.22	3.59	no
Subject 2	134.52	140.71	4.60	yes
Subject 3	158.40	155.83	-1.62	no
Subject 4	148.32	141.58	-4.54	yes
Subject 5	145.43	142.40	-2.08	no
Subject 6	157.29	154.33	-1.88	no
Subject 7	136.00	138.80	2.06	no
Subject 8	155.00	151.68	-2.14	no
Subject 9	147.73	149.77	1.38	no

The full effects of the artifact reduction strategy on median frequency are shown in Figure 3. Note that although the median frequency varied between subjects, within any given subject, the median frequency displays only small changes with artifact correction.

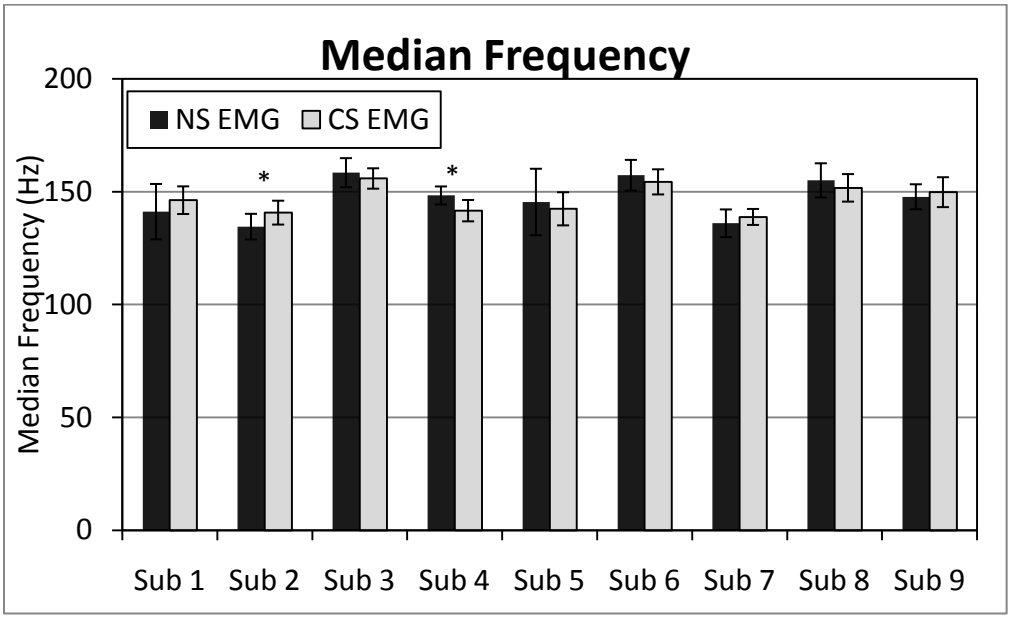

Figure 3: Average median frequency with and without scanning in the typical condition for each subject. Asterisks represent significant differences present at $p<0.05$.

When the effect of artifact reduction on power was evaluated, it was found that five subjects showed no significant change in power when comparing NS EMG with CS EMG, as shown in Table 4. The influence of artifact reduction ranged from subject to subject, with a percent change ranging from 1.7 to 65%.

Table 4: Average power values and changes with artifact correction

	Power (mV^2)			
	NS EMG	CS EMG	% Change	Significant at $p<0.05$
Subject 1	0.154	0.085	-44.94	yes
Subject 2	0.065	0.066	1.70	no
Subject 3	0.105	0.103	-2.38	no
Subject 4	0.083	0.050	-39.50	yes
Subject 5	0.096	0.034	-64.58	no
Subject 6	0.227	0.123	-45.85	yes
Subject 7	0.127	0.122	-4.09	no
Subject 8	0.061	0.043	-28.71	yes
Subject 9	0.063	0.075	19.15	no

It is noted that power is quite variable between contractions even within a single subject. The representative subject (Subject 6) had an average total power of $0.227mV^2$ with a standard deviation of 0.164 for the no scanning condition and an average total power of $0.123\ mV^2$ with a standard deviation of 0.065 for the scanning condition. Figure 4 shows the distribution of values obtained with the use of the function anova1 in Matlab when comparing total power for the representative subject in the scanning and no scanning conditions. This figure clearly demonstrates the variability in power for the representative subject as well as the dampening effect present with artifact correction.

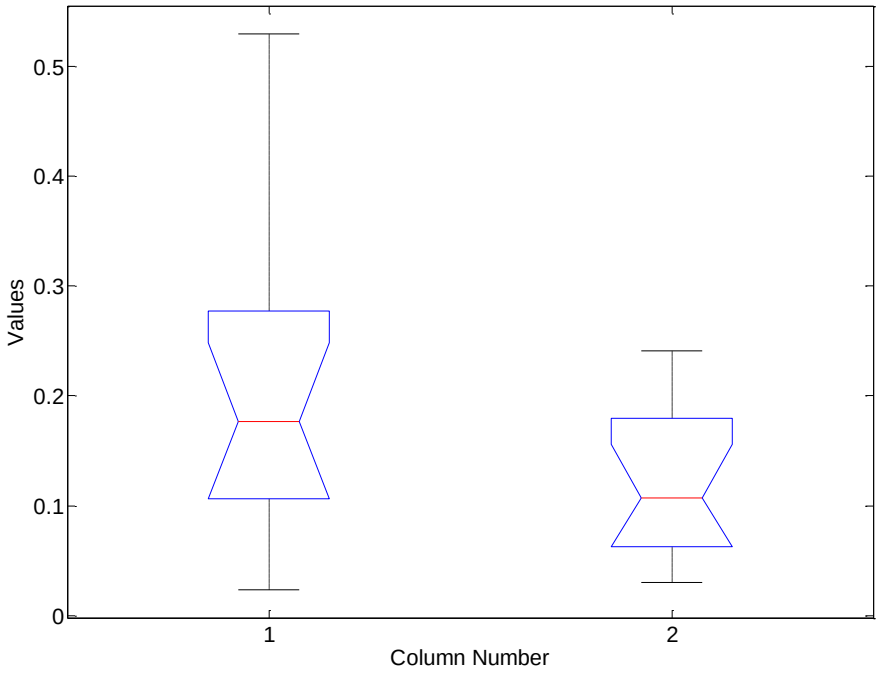

Figure 4: Box plot of total power values for the representative subject. Column 1: NS EMG; column 2: CS EMG

Power varied greatly between the subjects as well as within them. Figure 5 shows the variation in total power from subject to subject, ranging from over $0.2mV^2$ to approximately $0.05mV^2$.

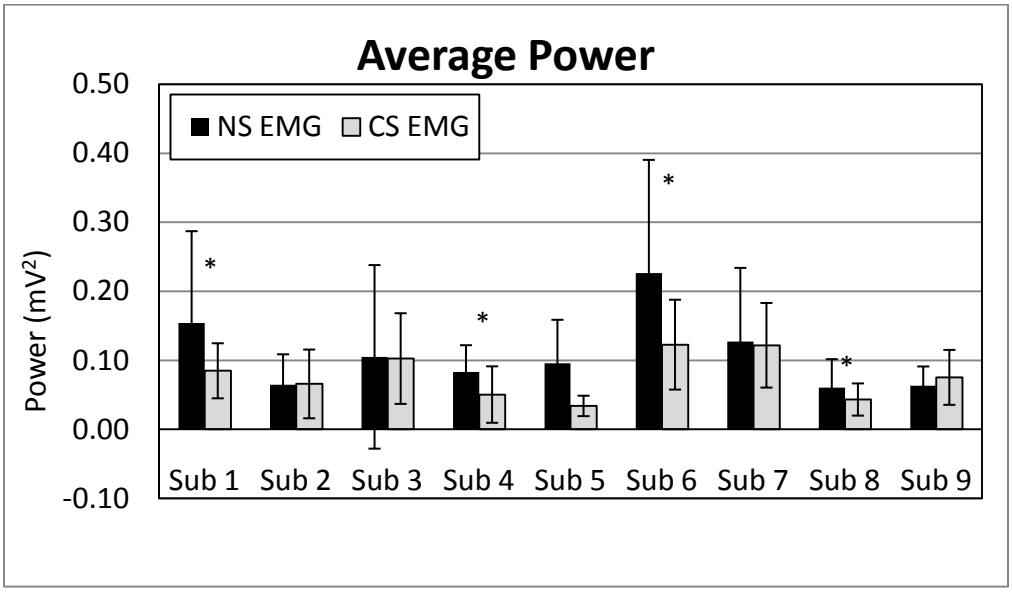

Figure 5: Average power values in the non-fatigued condition for each subject. Asterisks represent significant differences present at $p<0.05$.

The power spectrum of corrected EMG is very similar to the power spectrum of EMG collected with scanning, shown in Figure 6. Note that the general shape and proportions of the frequency spectrums match well. The full power spectrum indicates that although the total power was often significantly altered in the artifact reduction, the characteristics of the spectrum remained intact, which was indicated by the lack of change in median frequency.

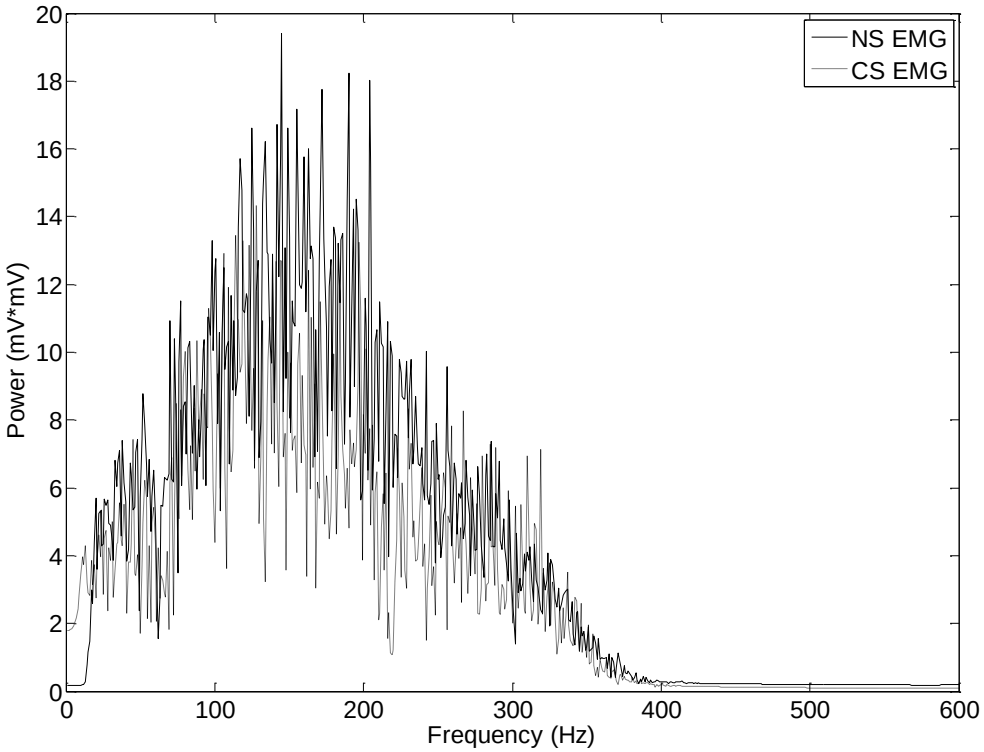

Figure 6: A typical power spectrum for EMG in the non-fatigued state with and without scanning

For inter-subject comparison, the effect of artifact reduction on amplitude was evaluated using root mean square (RMS) and normalization to the maximal voluntary contraction (MVC). A significant difference was present when comparing NS EMG with CS EMG for all subjects as seen in Table 5.

Table 5: Average amplitude by subject, normalized to the MVC and the changes with artifact correction

	Average Amplitude Normalized to the MVC			
	NS EMG	CS EMG	% Change	Significant at $p<0.05$
Subject 1	12.76	6.83	-46.44	yes
Subject 2	7.54	6.92	-8.18	yes
Subject 3	10.19	8.00	-21.45	yes
Subject 4	11.98	6.78	-43.42	yes
Subject 5	9.38	4.25	-54.66	yes
Subject 6	14.58	8.51	-41.65	yes
Subject 7	9.53	7.85	-17.63	yes
Subject 8	16.71	9.64	-42.31	yes
Subject 9	10.03	13.74	36.92	yes

A dampening effect was present in most (8/9) subjects as seen in Figure 7, though amplitude was consistent within the condition. For the representative subject (Subject 6), the amplitude of the NS EMG was 0.276 ± 0.026 mV, equivalent to 14.58% of the MVC and the amplitude of the CS EMG was 0.161 ± 0.005 mV, equivalent to 8.51 % of the MVC. Both conditions have low standard deviations.

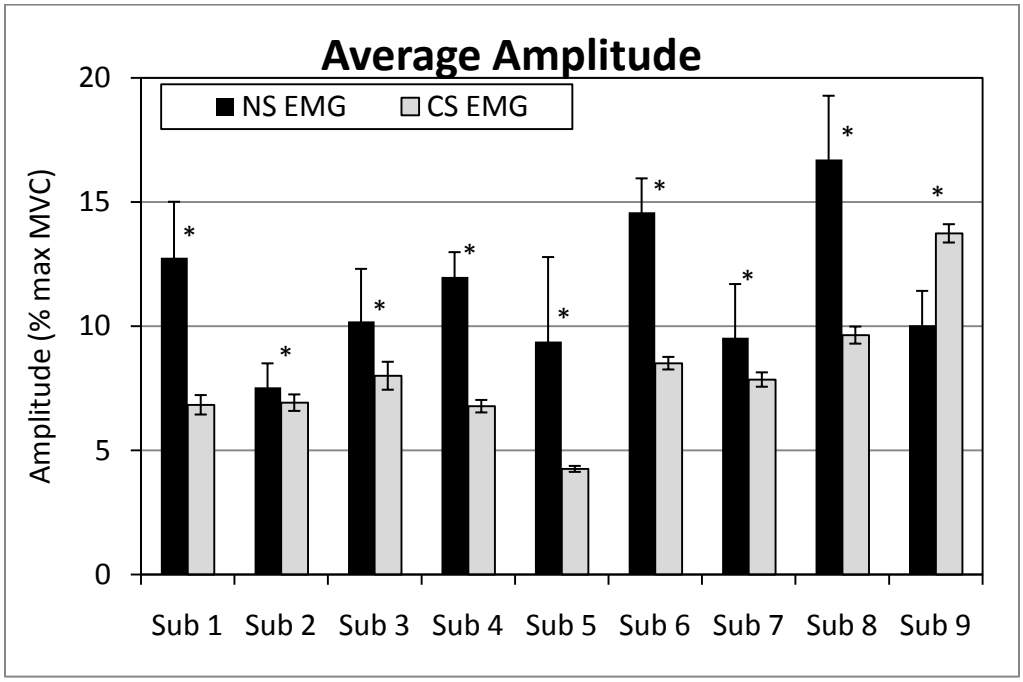

Figure 7: Average amplitude in the non-fatigued condition for each subject. Asterisks represent significant differences present at $p<0.05$.

Comparison of EMG parameters with no scanning and corrected with scanning showed that EMG parameters were not largely affected by artifact correction for most subjects. Median frequency was the parameter best retained. Though power was significantly different in several subjects, the large variability within the conditions is noted as well as the small sample sizes. Amplitude showed a consistent dampening effect with artifact reduction though amplitude was consistent within each condition.

4.4 Discussion

In order to effectively use an artifact reduction strategy, it is of upmost importance to fully understand how the data will be affected. Wavelet based artifact reduction retains

median frequency well. Only two subjects showed significant changes in median frequency when comparing NS EMG with CS EMG. It is believed that electrode placement may have played a role in the small but significant shift in median frequency present in these subjects. Remaining subjects showed no significant change in median frequency with artifact reduction. The high quality of the median frequency data is predominantly due to the development goals of this technique. As described in Chapter 3, thresholds were developed to maximize the retention of median frequency for the highest number of subjects possible. Although it was hypothesized that a significant shift in median frequency would be present in corrected EMG, the development goals of the methodology resulted in the negation of this hypothesis. By retaining the median frequency of EMG, this method retains the shape of the power spectrum so although the total power was influenced by artifact reduction in some cases, the characteristics of the spectrum remained largely unaffected.

In about half of the subjects, total power of the corrected EMG was significantly different from power of the EMG collected with no scanning. The high standard deviations are of particular note. Because of the high degree of variability in total power, coming to meaningful conclusions about significant changes resulting from artifact reduction is more difficult. It is speculated that the high standard deviations in total power may have related to small fatigue effects as variability in EMG power has been correlated with activity in brain areas linked to movement modulation (van Rootselaar et al. 2007b) and thus the deviations may have related to movement modulation. Due to the wide range in total power values, further studies should include a larger sample size of contractions for

analysis. Despite the shift in total power from NS EMG to CS EMG, the overall quality of the spectral characteristics is maintained. It is more important in EMG analysis to observe the shape of the power spectrum than to know the total power as the power spectrum provides information on the types of fibers active which can indicate muscular condition (Merletti and Parker 2004; Merletti et al. 1992). The hypothesis that wavelet based artifact reduction would have an influence on spectral parameters was shown to be true for total power.

EMG amplitude is often used use in clinical analysis for gait studies, biofeedback, neurological and neuromuscular evaluations (De Luca 1997). However, most EMG amplitude uses are qualitative instead of quantitative. The most common use of EMG amplitude is to demonstrate when a muscle is active or at rest. Amplitude is valued for providing timing information, which helps clinicians witness neuromuscular abnormalities by identifying whether a muscle is activating in correct sequence or if co-contraction is taking place. Wavelet based artifact reduction does have a significant effect on EMG amplitude in that a dampening effect was present. However, within a condition, the amplitude was consistent, with low standard deviations. This indicates that amplitude is still a reliable measurement post artifact correction. Aim 2 hypothesized that no change would be present in amplitude from NS EMG to CS EMG, however, in optimizing the methodology to retain median frequency, amplitude was dampened significantly.

An ideal artifact reduction would retain all EMG characteristics present in EMG collected without the artifact present. However, given the wide range of EMG parameters from subject to subject, an artifact reduction strategy intended to work well for a larger population must be optimized to a chosen parameter. The results presented in Chapters 3 and 4 and the thresholds described in Chapter 3 were optimized to retain median frequency in the largest number of subjects possible while removing as much artifact as possible. For clinical work with a single subject, thresholds could be easily modified to an individual's EMG characteristics for improved retention of all EMG parameters. Additionally, although median frequency was the EMG parameter chosen for optimization in this work, the thresholds could be modified, optimizing the methodology for different parameters, such as total power or amplitude. Wavelet based artifact reduction has been shown to effectively reduce artifact and retain good quality EMG in an MR environment.

Chapter 5: Assess the validity of wavelet denoising for EMG with atypical characteristics (Aim 3)

5.1 Introduction

The validation of an artifact reduction strategy for EMG collected during fMRI is very important. Users must know that the EMG retained post artifact correction is viable and reflects the underlying muscle activity. Current artifact reduction methods in this field have been validated using a wide range of methodologies (van Duinen et al. 2005; Allen et al. 2000; MacIntosh et al. 2007); none, however, have been tested in atypical conditions. Although it is certainly important to understand the influence artifact correction will have on the quality of EMG in typically developed subjects, it is equally important to understand several other factors. Is the artifact reduction robust? Even in typically developed subjects, EMG properties have a wide range of normal values so a robust technique is vital. Will artifact still be reduced in EMG with atypical characteristics? If EMG has atypical characteristics, will those usual characteristics be retained post artifact correction? These questions concern the value of an artifact correction strategy in a clinical setting. Additionally, significant changes in muscle activity must be identifiable. Without the ability to detect changes it is difficult to gauge progress in patients. In neuroplasticity studies, increases in the volume of the cortex activated are touted as evidence of successful therapies. Yet no motor studies on neuroplasticity have explained what changes in cortical activations mean (Phillips 2007). With the ability to detect changes at the muscle level, a better understanding of cortical changes can be gained.

Aim 3 focuses of validating wavelet based artifact reduction for EMG during an fMRI in an atypical condition. Fatigued muscle has very distinct EMG characteristics and fatigue can be easily generated in a typically developed population. The methodology described in Chapter 3 will be evaluated in this chapter for how well it functions in EMG with distinctly different characteristics from typical EMG. Just as the quality of the typical post correction EMG was established in Chapter 4, the quality of the fatigued EMG post correction must also be assessed. Furthermore, changes present with fatigue in a non scanning environment must be evaluated and compared with changes present with fatigue in the post correction EMG. This chapter discusses wavelet based artifact reduction in an atypical condition and evaluates the methodology for retaining and detecting small but significant changes in muscle activity.

5.2 Methods

Subjects

The subject population was the same as used in Chapter 3.

Experimental Protocol

The experimental protocol used in Chapter 3 provided baseline measurements. The following protocol was included to provide atypical, fatigued measurements. Before the experiment started, subjects practiced the motor task. The tasks consisted of a series of rests, strong sustained contractions, and ankle movements through the full range of motion at a self-selected pace. The experimental design protocol utilized a basic block design with 4 repetitions per experiment and 10 measurements per block. A sequence of

rest, sustained contraction, and then ankle movements was performed and repeated four times. Rest and ankle movement blocks were 30 seconds in duration. The sustained contraction, designed to fatigue the anterior tibialis muscle to a moderate degree but leave the muscle able to recover during the rest period, was 60 seconds in duration. Complete, this experiment lasted a total of eight minutes. Verbal instructions to rest, begin movement, or sustain the contraction were provided by the fMRI technician through headphones. The head was immobilized using foam pads and tape. The ankle was supported by a pillow to enable a full range of motion without moving the leg. Prior to scanning, the subject practiced the task while inside the scanner to confirm EMG setup and ensure the subject was comfortable with the instructions before beginning data collection and introducing fMRI artifact into the EMG. Three maximal voluntary contractions (MVCs) were performed, lasting approximately two seconds each with up to 20 seconds of rest between them.

All tasks were performed twice, once without fMRI scanning for baseline EMG measures while the subject was within the scanner, and once with fMRI scanning. In addition to creating artifact to develop and test the artifact reduction technique, fMRI scans were performed to confirm that the quality of the fMRI images would not be disturbed by the EMG equipment and to assess the value of including EMG parameters in the analysis of the images.

fMRI Measurements

FMRI measurements for unfatigued baseline measures were the same as described in Chapter 3. fMRI scans for the fatigue experiment were set up identically. The only change was the inclusion of the sustained contraction blocks.

EMG Measurements

EMG measurements were collected as described in Chapter 3.

EMG Processing

EMG was processed as described in Chapter 3. Post artifact correction, bursts of EMG activity were analyzed individually for amplitude by root mean square, median frequency, and total power. This was done to show the expected range for each parameter for each subject in a given condition. All values for a given parameter in a condition for a subject were found and combined to increase the power of statistical analysis. Mean values and standard deviations were found for each EMG parameter. Percent differences were calculated to establish what effects were present with this artifact reduction strategy in place.

Statistics

Complete validation of the artifact reduction strategy included assessment of how well the artifact reduction strategy removed artifact and retained EMG characteristics in fatigue, an atypical condition. For Hypothesis 3.1 and 3.2, an ANOVA for repeated measures was performed to compare the NS EMG with the NSF EMG to identify the

distinct changes that take place during fatigue conditions and introduce a baseline for comparison. The average amplitude, median frequency, and total power were found for each subject in each condition. Each EMG burst was analyzed and combined to produce a distribution for each parameter for each condition (no scanning, scanning) in each subject. Amplitude, median frequency, and total power were all assessed to establish if significant changes were present and percent change was found for amplitude and total power though actual change was used for median frequency. An ANOVA for repeated measures was also performed to compare the CS EMG with the CSF EMG to identify what distinct changes occurred between these conditions. The same analysis taking place for identifying changes with fatigue in the no scanning condition was applied to the scanning condition EMG. The results of the typical and fatigued analysis were compared from the no scanning condition to the scanning condition, with all parameters being assessed. Percent change was calculated for amplitude and total power and change was calculated for median frequency.

5.3 Results

To assess the development of the artifact correction strategy in an atypical condition, EMG from a representative subject (Subject 6) is presented in Figure 8. Without scanning, EMG activity is clear with five contractions taking place within 25 seconds. It is noted that the amplitude of the contractions is lower overall than in the unfatigued condition presented in Chapter 3 for the same subject. EMG collected during scanning is very noisy. It is difficult to identify muscle contractions and the artifact is obscuring valuable data. Post artifact correction by wavelet denoising nearly all visible artifact has

been removed and muscle activity is evident, with distinct contractions though a dampening effect on the amplitude is present.

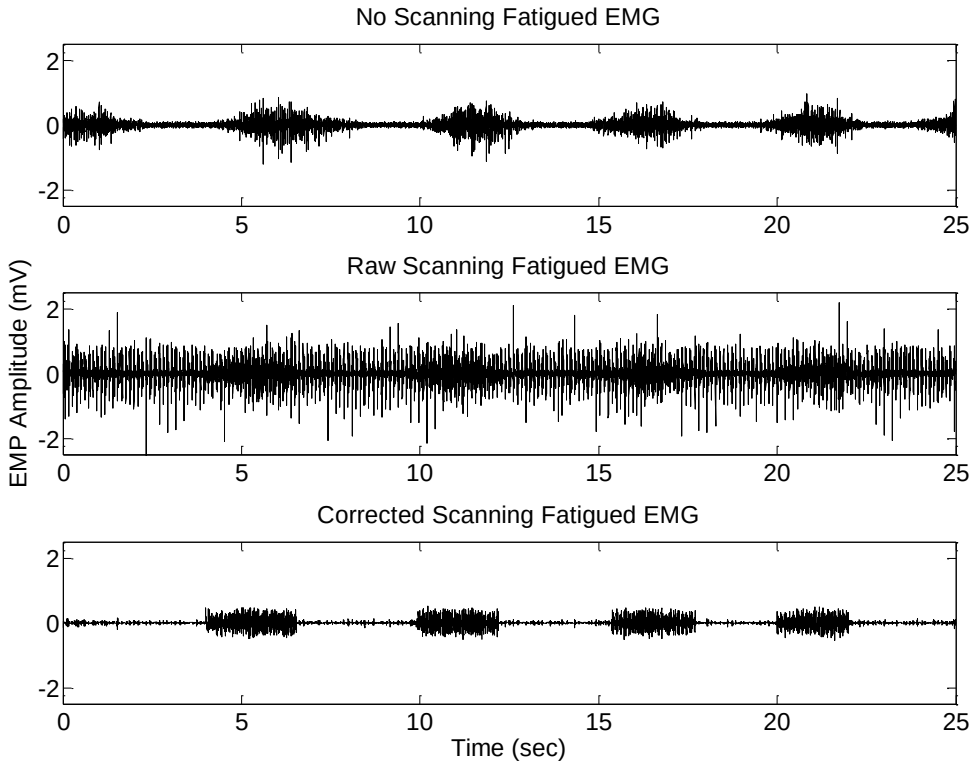

Figure 8: EMG from a representative subject in the fatigued condition from a repetition without scanning (top), and a repetition with scanning pre (middle) and post (bottom) artifact correction

Baseline changes in no scanning EMG with fatigue were evaluated for each subject. No significant changes were found with fatigue in a direct comparison of the signals for any subject. Three subjects (subjects 1, 2, and 5) showed no significant change in median frequency in the fatigue condition, indicating that no fatigue took place in these subjects.

All other subjects demonstrated significant changes in median frequency with fatigue, generally a shift down. Significant changes in power did not occur with fatigue in most subjects in the no scanning condition. Changes in amplitude followed no particular trend with some subjects showing significant shifts with fatigue while others presented with no significant change.

In evaluating the artifact reduction strategy in an atypical condition, changes presented in the no scanning fatigue condition were compared with changes that occurred with fatigue in the corrected scanning EMG. No significant differences were found in a direct comparison of the signals for any subjects, just as in the no scanning condition.

Median frequency analysis showed that, as seen in Table 6, the second condition was appropriately identified for each subject. Subjects who showed no fatigue (indicated by no significant change in median frequency) in the no scanning condition also showed no fatigue in the scanning condition. All subjects who fatigued and entered a second muscular condition in the no scanning condition showed the same significant change in the scanning condition. Significant changes in median frequency for the no scanning condition ranged from approximately 6 to 14Hz while changes in the scanning condition post artifact correction ranged from approximately 3 to 9Hz. Thus, although a slight dampening effect is present with artifact correction, significant shifts in median frequency mirror those taking place in the no scanning condition.

Table 6: Median frequency changes with fatigue in scanning and non scanning conditions. Note that very low changes in median frequency (Subjects 1, 2, 5) corresponded with no significant differences in the data sets.

	Median Frequency (Hz)							
	NS EMG	NSF EMG	CS EMG	CSF EMG	Change NS	Change CS	Significant at p<0.05 NS	Significant at p<0.05 CS
Subject 1	141.15	139.59	146.22	146.87	-1.55	0.64	no	no
Subject 2	134.52	132.64	140.71	141.98	-1.87	1.27	no	no
Subject 3	158.40	151.71	155.83	152.07	-6.69	-3.77	yes	yes
Subject 4	148.32	134.72	141.58	135.29	-13.59	-6.28	yes	yes
Subject 5	145.43	131.00	142.40	142.50	-14.43	0.10	no	no
Subject 6	157.29	144.47	154.33	149.15	-12.82	-5.18	yes	yes
Subject 7	136.00	125.44	138.80	134.50	-10.56	-4.30	yes	yes
Subject 8	155.00	146.76	151.68	155.08	-8.24	3.39	yes	yes
Subject 9	147.73	155.54	149.77	140.90	7.81	-8.87	yes	yes

Histograms of the median frequencies present for each contraction in each condition for a representative subject (Subject 6) are shown in Figure 9, displaying the shift in median frequency that is present in both no scanning and scanning conditions with fatigue. Note the clear shift to lower median frequencies in the fatigue state.

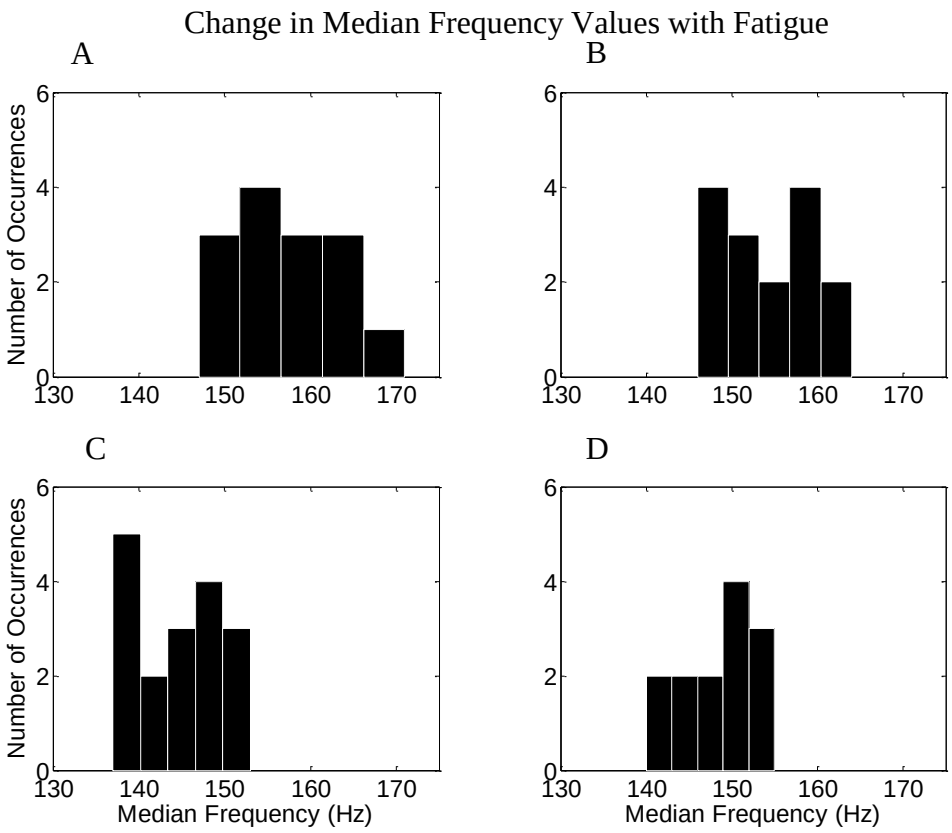

Figure 9: Histogram of median frequency values of a representative subject for A) NS EMG B) CS EMG C) NSF EMG and D) CSF EMG

An analysis of the total power in unfatigued and fatigued conditions showed that no significant change was present in most subjects with fatigue. The lack of significant change in total power with fatigue in the no scanning condition was mirrored in the corrected EMG. The percent change in total power did vary considerably as seen in Table 7. In a representative subject (Subject 3), no significant change in total power was present with fatigue in the no scanning and scanning conditions. The percent change was higher in the no scanning condition, at about a 50% decrease, while in the scanning condition the total power increased approximately 6% on average. The mean for the NS

EMG was 0.1050mV^2 with a standard deviation of 0.1330; with fatigue, the mean shifted to 0.1267mV^2 with a standard deviation of 0.0958. In the scanning condition, the CS EMG had a mean of 0.1025mV^2 with a standard deviation of 0.0657; with fatigue, the total power shifted to 0.1243mV^2 with a standard deviation of 0.0652. This shift was found to not be significant at the $p<0.05$ level. Note that the standard deviations are at similar levels.

Table 7: Power changes with fatigue in scanning and non scanning conditions

	Power (mV^2)							
	NS EMG	NSF EMG	CS EMG	CSF EMG	% Change NS	% Change CS	Significant at p<0.05 NS	Significant at p<0.05 CS
Subject 1	0.154	0.100	0.085	0.090	-34.81	5.78	no	no
Subject 2	0.065	0.065	0.066	0.068	0.77	2.89	no	no
Subject 3	0.105	0.127	0.103	0.124	20.67	21.27	no	no
Subject 4	0.083	0.064	0.050	0.048	-23.65	-4.37	no	no
Subject 5	0.096	0.202	0.034	0.089	110.76	161.95	no	yes
Subject 6	0.227	0.110	0.123	0.130	-51.46	5.79	yes	no
Subject 7	0.127	0.135	0.122	0.154	6.46	26.77	no	no
Subject 8	0.061	0.040	0.043	0.033	-34.32	-24.07	no	no
Subject 9	0.063	0.058	0.075	0.048	-8.86	-36.79	no	no

The results of the amplitude analysis are shown in Table 8. Amplitude follows no specific pattern in this test though subjects were asked to perform contractions at near maximal levels. The percent change in amplitude present with fatigue was consistently higher in the no scanning condition. The dampening effect on amplitude discussed in the previous chapter is also present in the fatigued state.

Table 8: Amplitude changes with fatigue in scanning and non scanning conditions

	Amplitude Normalized to the MVC							
	NS EMG	NSF EMG	CS EMG	CSF EMG	% Change NS	% Change CS	Significant at p<0.05 NS	Significant at p<0.05 CS
Subject 1	12.76	8.72	6.83	6.60	-31.68	-3.40	yes	yes
Subject 2	7.54	6.69	6.92	6.85	-11.18	-0.99	yes	no
Subject 3	10.19	10.93	8.00	8.00	7.30	-0.07	no	no
Subject 4	11.98	11.37	6.78	6.92	-5.12	2.03	no	no
Subject 5	9.38	10.33	4.25	4.22	10.06	-0.71	no	no
Subject 6	14.58	9.88	8.51	8.06	-32.27	-5.24	yes	yes
Subject 7	9.53	9.10	7.85	7.66	-4.54	-2.39	no	no
Subject 8	16.71	15.30	9.64	9.28	-8.47	-3.74	no	yes
Subject 9	10.03	8.23	13.74	13.88	-18.02	1.00	yes	no

With wavelet based artifact correction, the changes present with fatigue included a downward shift in median frequency, no significant change in a direct comparison of the signals, generally no change in total power, and no consistent change in amplitude. These changes mirror the changes present in EMG with fatigue without fMRI scanning.

5.4 Discussion

The artifact reduction technique presented in this work is the first to be evaluated in an atypical condition. This work demonstrates that wavelet based artifact reduction remains viable in a second condition. Artifact is reduced, high quality EMG is retained, and the EMG changes associated with the second condition are correctly identified. These all indicate the value of wavelet based artifact reduction in combined EMG and fMRI studies.

FMRI motor fatigue studies have begun utilizing concurrent EMG in recent years as the techniques for collecting EMG in the MR environment have improved (Bigland-Ritchie et al. 1983; van Duinen et al. 2007; Benwell et al. 2006; Liu et al. 2003; Liu et al. 2005; Post et al. 2008). However, fatigue conditions result in EMG with atypical spectral characteristics. Therefore, without an analysis of how well the artifact reduction strategy works in fatigue conditions, the EMG analysis presented in such articles is not assured to be valid. One purpose of this work is to correct that oversight. With the presented validation, wavelet based artifact reduction for EMG can be used in future motor fatigue studies with confidence.

With wavelet based artifact reduction, in the typical condition the median frequency was retained for most of the population and this was again true in the fatigued state. Similar shifts in median frequency occurring with changes in muscle state were witnessed in the no scanning and corrected scanning conditions. The histograms of the median frequency distribution for each condition in the representative subject demonstrate the downward shift in median frequency, exactly as expected with fatigue (Merletti and Parker 2004) in both the no scanning condition as well as in the corrected scanning data. This witnessed shift confirms that fatigue has occurred in both conditions and that the fatiguing exercise produced consistent degrees of fatigue within a subject. Our hypothesis that EMG parameters in fatigued muscle would be unchanged from no scanning to corrected scanning EMG was found to have mixed results. Median frequency was retained effectively though power was not as consistent in the two conditions and amplitude was

again dampened. This finding was consistent with the findings in Chapter 4 and the optimization of the technique for the retention of median frequency.

Wavelet based artifact reduction allows for the identification of typical and fatigued muscle conditions. This is demonstrated by the correct identification of fatigue in each subject. The three subjects who did not significantly fatigue in the scanning condition were correctly evaluated, as confirmed by also not showing fatigue in the no scanning condition. This demonstrates that the median frequency of EMG is correctly retained, and that it is possible to correctly track motor fatigue in the MR environment. This also shows our hypothesis that frequency parameters would shift according to fatigue in the corrected scanning condition was shown to be correct with respect to median frequency. It is believed that the subjects who did not show muscular fatigue were not performing the sustained contraction at maximal levels. Though cortical fatigue effects were visible, as will be discussed in Chapter 6, at the level of the muscle, those three subjects did not present with significant fatigue. This result provides evidence that wavelet based artifact reduction does in fact allow for the distinction between muscular conditions in the MR environment. As correctly identifying changes in muscle state is critical for the analysis of therapies, this finding indicates that value of wavelet based artifact reduction in clinical studies.

Not only does wavelet based artifact reduction retain median frequency well enough to distinguish between muscular conditions, the artifact reduction is still effective in the second condition. Artifact is reduced in the fatigue condition just as effectively as in the

unfatigued state. Power is still well retained and amplitude is again dampened consistently. Wavelet based artifact reduction is currently the most robust strategy validated for reducing artifact in EMG collected during fMRI. With the knowledge that the artifact will be reduced and key EMG parameters retained during analysis, wavelet based artifact reduction is the best tool to use with clinical fMRI studies. Many neuromuscular conditions are characterized by atypical muscle activity; therefore, it is crucial to have a robust method for reducing the artifact in such cases. Though previous methods, specifically the Allen method, are being used in atypical conditions, there is no assurance that artifact is being removed well, EMG parameters retained, and significant differences from typical EMG retained.

This work demonstrates that wavelet based artifact reduction is effective for atypical muscle activity. Artifact is reduced and good quality EMG is well retained. In fatigue conditions, median frequency is tracked successfully, introducing new options in the design of motor fatigue studies. Most importantly, wavelet based artifact reduction allows for small but significant changes in EMG to be witnessed. Therefore, not only can muscular conditions be distinguished, but progress can be tracked in clinical studies. This will allow for changes to be monitored at both the muscular and cortical levels in neuroplasticity studies. Wavelet based artifact reduction is the only artifact reduction strategy currently validated for tracking changes and distinguishing between muscle conditions. This novel work introduces new capabilities into fMRI studies that will begin to answer many fine motor control questions.

Chapter 6: Assess of the effects of EMG parameters as regressors in the analysis of motor fatigue on cortical activation during voluntary ankle movements (Aim 4)

6.1 Introduction

FMRI studies can provide valuable information about cortical control in motor studies. Although there is no dispute about the value of collecting EMG during fMRI studies, if the quality of the fMRI or EMG data is compromised, the combined modalities are not successful. Certainly with the development of a new artifact reduction strategy for any type of signals that will be collected during fMRI, the effects of the artifact reduction on the desired signal must be well understood. As seen in chapters 4 and 5, high quality EMG can be retained during fMRI studies with the use of wavelet based artifact reduction. However, it is of equal importance to still obtain high quality fMRI data. Hardware used for electrophysiological signal collection must be carefully selected to maintain safety and minimize the influence on fMRI scanning as discussed in Chapters 2 and 3. Even with careful selection of hardware, to evaluate if the EMG data collection negatively impacts the fMRI study, full analysis of cortical activations must be performed.

In this chapter, Aim 4 explores the quality of the fMRI results collected simultaneously with EMG. A basic motor task of ankle dorsiflexion and plantarflexion allows for the comparison of the results of this study with those established in the literature. The inclusion of a motor fatigue task will further test the quality of fMRI data. Cortical activation over the course of motor fatigue is well documented and will provide a basis for comparison. This chapter includes a complete analysis of the fMRI data in both

unfatigued and fatigued states to demonstrate the high quality of the fMRI results despite the inclusion of EMG.

With the quality of the fMRI analysis confirmed, this chapter will also examine the advantages of combined modalities. One challenge in fMRI motor fatigue studies is that because individuals fatigue so differently and fatigue is difficult for subjects to report due to its qualitative nature, fMRI motor fatigue study design has been limited to fatiguing subjects to exhaustion. With EMG collection, motor fatigue can be quantified using the change in median frequency as a fatigue index. This chapter will explore the inclusion of change in median frequency as a covariate to account for variation in individual fatigue. Aim 4 confirms high quality fMRI data is being collected with EMG and examines one method by which fMRI studies may be enhanced with EMG.

6.2 Methods

Subjects, experimental protocol, EMG measurements, EMG processing, and fMRI measurements were the same as described in Chapters 3 and 5.

fMRI Analysis

FMRI data were analyzed using a standard Statistical Parametric Mapping software (SPM8) in Matlab 7.1. All functional images were aligned, normalized to a standard echo planar image, and smoothed using two times the voxel size. In the first level analysis, global normalization was used with a scaling function and a high-pass filter of

128Hz was chosen. To account for head movement, the movement parameters were included as multiple regressors (Johnstone et al. 2006). Subjects with head movement exceeding 3 mm were not included in the analysis (1 subject). The general linear model (GLM) incorporated in SPM to analyze BOLD data was modeled using a canonical hemodynamic response function and a Student's t-test was performed to find active areas using a contrast in which activations during rest periods were subtracted from activations during ankle movement periods.

In the second level analyses group-level random effects analyses for main effects were accomplished by entering whole brain contrasts into one-sample t-tests. A significance threshold based on spatial extent using a cluster probability of a corrected ($p \leq 0.001$) and spatial extent > 10 voxels was applied to the effects of interest and surviving voxels were retained for further analyses. The typical condition (no fatigue), and the fatigue condition were processed similarly with no covariates. However, the group fatigue condition was also analyzed using the change in EMG parameter median frequency, obtained from the EMG analysis, as a covariate to account for variations in fatigue between subjects. The intersection of the left hemisphere with Brodmann's area 4 and the supplementary motor area were identified as the regions of interest and images were masked accordingly using Pickatlas (Maldjian et al. 2003; Maldjian et al. 2004).

6.3 Results

In the evaluation of the quality of fMRI data when EMG collection was taking place, first level analysis of a single subject showed strong cortical activations. A representative subject is shown in Figure 10 with no masking to show the full range of cortical activation present in the unfatigued ankle movements. Note that in this basic motor task of right ankle dorsiflexion and plantarflexion with a threshold of p=0.001, cortical activation is strong, predominantly in the left hemisphere, and in primary and supplementary motor areas (cross hair). The images are represented in neurological coordinate system (left of the image corresponds to the left hand side of the subject).

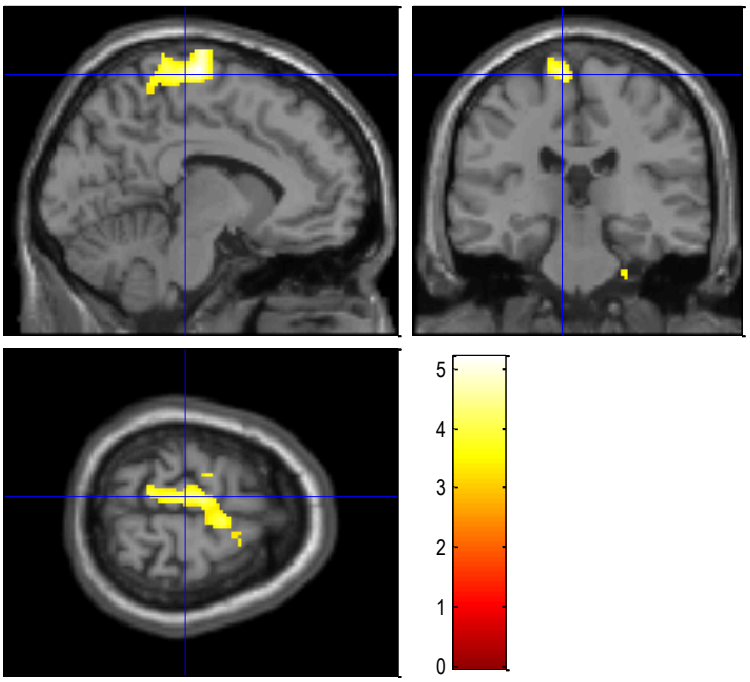

Figure 10: Cortical activations for a single subject during unfatigued right ankle movements

The group analysis shows similar results. In the unfatigued condition, as seen in Figure 11, cortical activation is seen in the left motor cortex in primary and supplementary motor areas.

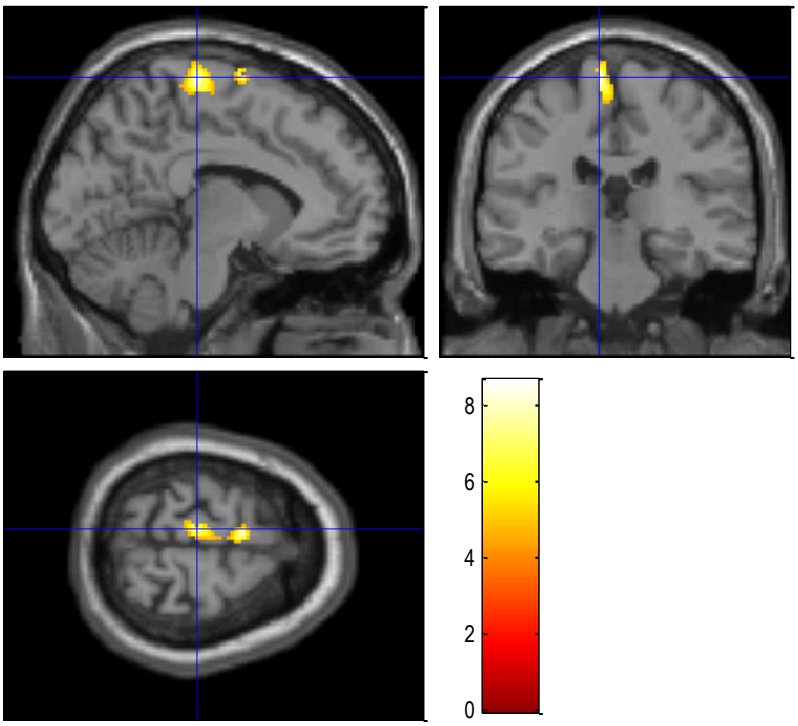

Figure 11: Group results for cortical activations during right ankle movements in the unfatigued condition. Images are masked to for motor areas in the left hemisphere

A motor homunculus (Blumenfeld 2002) is shown in Figure 12 for comparison. Note the region activated in Figure 11 (cross hair) corresponds with the region for the lower leg, ankle, and foot in the homunculus.

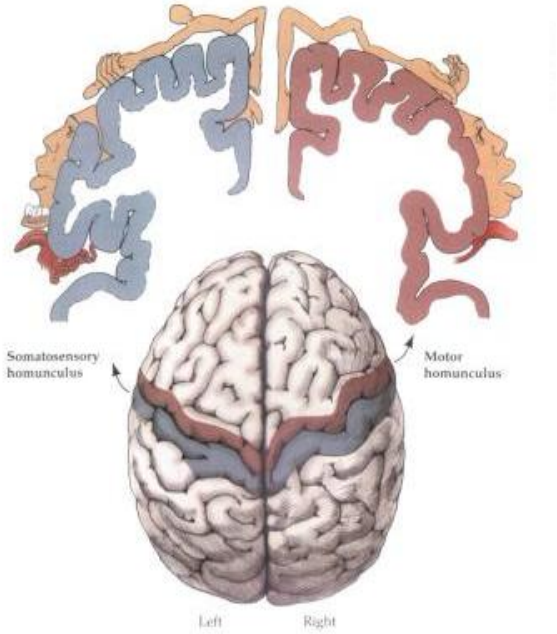

Figure 12: Somatosensory homunculus (Left) and motor homunculus (right) showing regions of the cortex that correspond with sensation or motor control of the body
(Blumenfeld 2002)

Volumetric measurements of the cortical activation areas based on the region of interest measurements show that in the unfatigued condition, a volume of 2592mm^3 was active at the p value of 0.001 in the left hemisphere with masking for Brodmann's Areas 4 and 6. The center of the activation is shown in Table 9 with the Z score, regions active, and volume active.

Table 9: Location, volume and z-score of cortical activations in the typical condition, fatigued condition, and the fatigued condition with the inclusion of change in median frequency as a covariate

	Group Analysis					
	Location (MNI)			Location Description	Z score	Volume Active (mm^3)
Typical	-5.84	-19.80	69.00	Left Hemisphere M1, SMA	4.22	2592
Fatigue	-11.80	-21.70	70.00	Left Hemisphere M1	3.53	200
Fatigue with Median Frequency	-11.70	-21.90	70.40	Left Hemisphere M1	3.44	160

In the group analysis of the fatigue condition, cortical activation was again located in the left motor cortex as shown in Figure 13. However, the volume active was greatly decreased at 200mm^3. Note that although the volume is considerable decreased, the active region is again associated with left leg movement.

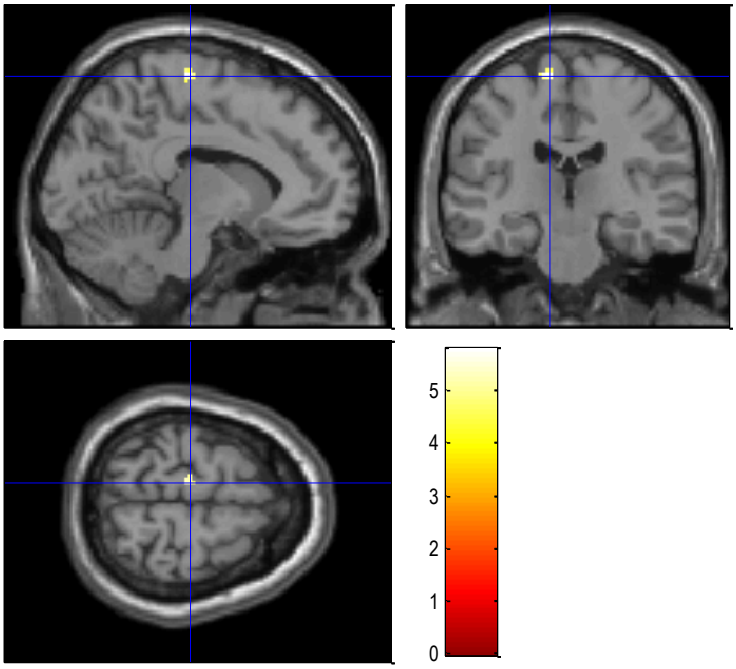

Figure 13: Group results for cortical activations during right ankle movements in the fatigued condition. Images are masked for motor areas in the left hemisphere

In the evaluation of using EMG parameter median frequency as a random effects variable, the group analysis for fatigue conditions was performed with the change in median frequency as a covariate and the resulting cortical activation map shown in Figure 14.

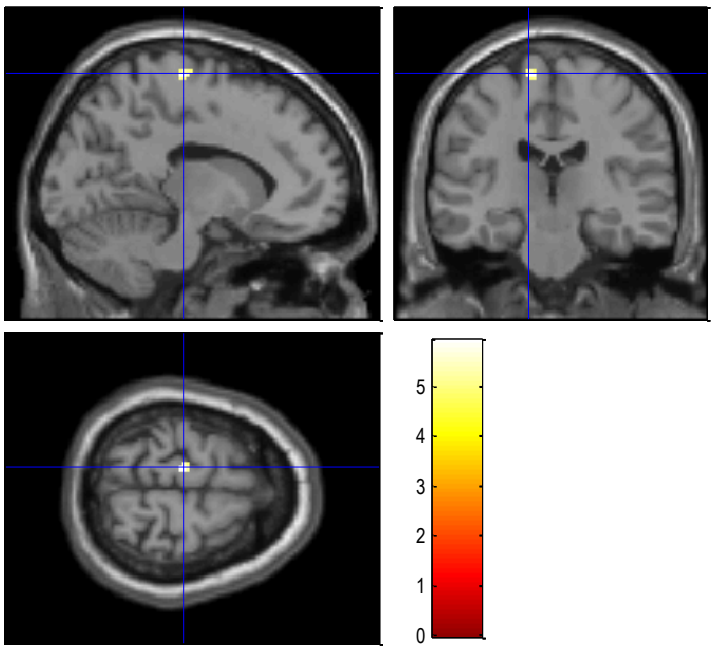

Figure 14: Group results for cortical activations during right ankle movements in the fatigued condition with the inclusion of change in median frequency as a covariate. Images are masked for motor areas in the left hemisphere

The location of the activation as well as the volume active is displayed in Table 9. Note that the region active in both fatigue condition analyses is nearly identical. However, with the inclusion of median frequency as a random effects variable, the volume active decreases from 200mm^3 to 160mm^3. The overall results of fMRI analysis with EMG data collection are shown in Figure 15 and Table 9.

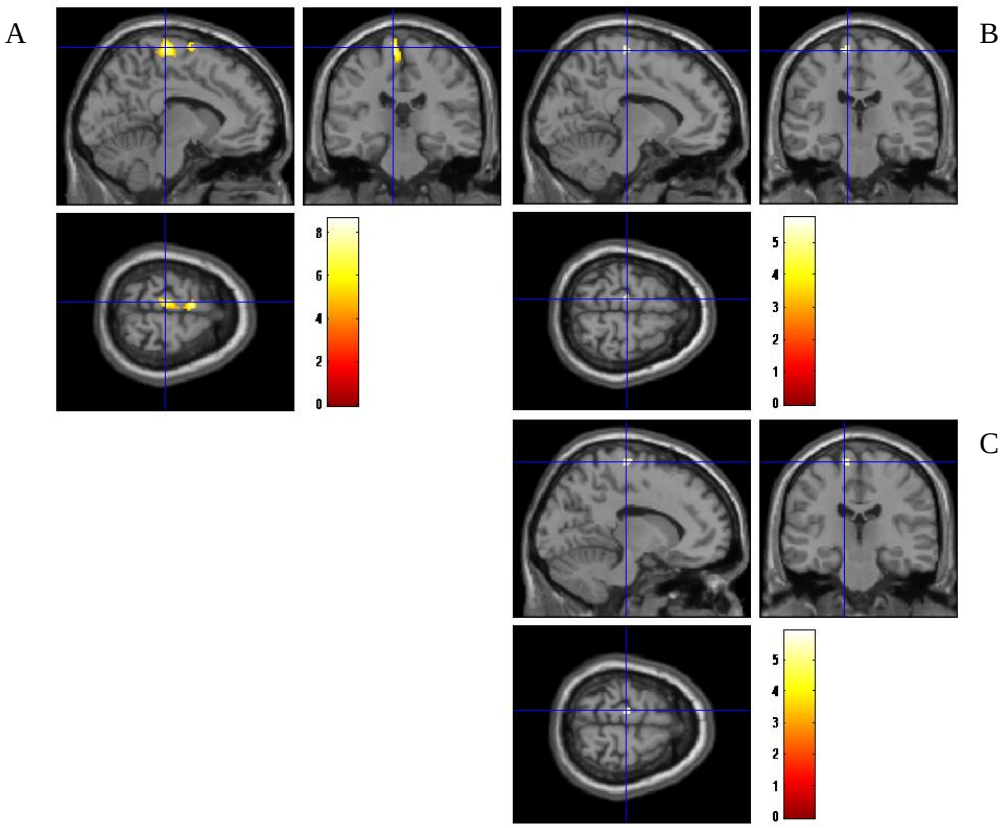

Figure 15: Activation Maps for the Group Analysis in the A) Typical Condition B) Fatigued Condition and C) Fatigued Condition with the inclusion of change in median frequency as a covariate

6.4 Discussion

In any fMRI study, high quality fMRI results are paramount. When combining fMRI with other technologies such as EMG, there is the potential that recording equipment may interfere with the magnetic fields, reducing the quality of the fMRI results. Establishing that fMRI data collection is not compromised by the inclusion of EMG measurements is therefore of vital importance. Without high quality fMRI and EMG, the combined modalities effort has failed. However, once both high quality fMRI and EMG can be

obtained simultaneously, new approaches and opportunities to understanding fine motor control may be explored and existing experimental designs may be refined. The use of EMG in fMRI analysis has been used in several studies (van Rootselaar et al. 2007b; van Duinen et al. 2007) but this chapter expands upon current studies by including EMG parameter median frequency as a random effects variable in a motor fatigue study.

The evaluation of the quality of fMRI data collected simultaneously with EMG demonstrated that cortical activations were as expected for right ankle dorsiflexion and plantarflexion. In the representative subject with no masking, strong activations were present at the threshold of p=0.001. Activations were predominantly on the left side of the brain in motor areas, as expected for right ankle movements, however some activation was witnessed in the right hemisphere. This coactivation is not unusual given the strength of the signal for a basic motor task and might have been contributed during mirror neuron effects as well.. When compared with the motor homunculus, it is clear that the region of the motor strip active in this study is associated with lower leg and ankle movements, further confirming the high quality of the fMRI results. Many motor studies have used ankle dorsiflexion and plantarflexion and thus our results can be compared to established findings in the literature. A recent study compared cortical activations during active, passive and electrically stimulated right ankle movements (Francis et al. 2009). The motor task, experimental protocol, and fMRI image processing were all similar to the work presented here. During active right ankle movements, the strongest activations were witnessed in the contralateral primary motor and primary sensory cortex as well as the supplementary motor area (Francis et al. 2009). In comparison, the work presented here showed significant activations in the contralateral

motor cortex and the contralateral supplementary motor area. It is noted that masking was used in the work presented here to only show motor areas. However, despite differences in masking, both studies showed remarkably similar results for actively controlled right ankle movements. This comparison provides strong evidence that the quality of fMRI data collected simultaneously with EMG was not compromised.

Although the unfatigued fMRI data was found to be valid with simultaneous EMG collection, by examining the changes in cortical activation present with motor fatigue, further verification of the high quality of fMRI data can be performed. Cortical activation patterns with motor fatigue have been well established. Several studies have documented an initial increase in the volume active with motor fatigue followed by an overall decrease in the active volume (Liu et al. 2002; van Duinen et al. 2007; Benwell et al. 2006; Liu et al. 2003; Liu et al. 2005). The results presented in this work correspond with established patterns. When comparing the unfatigued and fatigued cortical activation maps, the active volume decreases from 2592mm^3 to 200mm^3. As the findings correspond with patterns established in the literature, the high quality of the fMRI data cannot be in doubt. This significant decrease in active volume also demonstrates that the experimental design presented here was appropriate to fatigue the subjects at a cortical level.

One feature of the experimental design used in this study was that subjects did not fatigue identically. Fatiguing two people identically to a moderate level is very difficult. Without EMG, fatigue is very qualitative and difficult to compare between people. Even

with EMG collection and the calculation of median frequency to use the change in median frequency as a fatigue index, only muscular fatigue effects can be witnessed. Because individuals fatigue differently at both the muscular and cortical level, a great deal of variation is present in both the median frequency changes of the EMG and the volume active in the fMRI results. By accounting for variations in individual fatigue at the muscle level, this study attempted to improve cortical analysis. When the average change in median frequency for each individual was used as a fatigue index and included as a random effects variable in the group analysis, the volume of cortex active decreased. The center of activation was nearly identical, indicating that the analysis was refined but not overly influenced by the inclusion of change in median frequency as a random effects variable. This verifies the hypothesis that including the individual fatigue index as a random effects variable has a significant impact on fMRI analysis. By including a fatigue index in the cortical analysis, a better understanding of fatigue can be gained for the population. Additionally, by accounting for individual variations in fatigue during a motor task, motor studies might also be enhanced. This work demonstrates how valuable the inclusion of EMG with an effective and flexible artifact reduction strategy can be. Not only can we obtain valuable information about muscle activity and muscle state during neuroimaging studies with this methodology, but we can apply this information to improve our understanding about cortical activations and motor control. Wavelet based artifact reduction of EMG will be a tool used in the pursuit of fine motor control questions in which small differences in muscle state may influence the results of the study.

Chapter 7: Conclusions

Wavelet based artifact reduction introduces new capabilities into fMRI studies. This method effectively reduces artifact from EMG while retaining key EMG characteristics and parameters without the use of combined repetitions or smoothing. This artifact reduction is accomplished with a very robust methodology which allows imaging protocol to be optimized. The preliminary work for this study was performed in a 1.5 Tesla scanner and translated to a 3 Tesla scanner, suggesting this methodology is adaptable without sacrificing quality, a valuable asset. With wavelet based artifact reduction, small but significant changes in muscle activity and state are now visible in the MR environment. Muscle fatigue was correctly identified in all subjects with shifts in median frequency up to 5%. This shift indicates a change in muscle state and introduces the possibility of expanding motor fatigue study design. When fatigue parameters found with EMG analysis were included as a random effects variable during second level analysis of fMRI data, the results were refined. This finding demonstrates the value of including good quality EMG parameters in cortical analyses to account for variance in a population. Additionally, the ability to track small changes in muscle activity indicates that this methodology will be useful in neuroplasticity studies to relate changes in muscle performance to cortical activation shifts. Wavelet based artifact reduction allows for high quality EMG to be retained in the MR environment and applied to improve our understanding of cortical activation.

Although this work demonstrates that wavelet based artifact effectively reduces artifact in EMG collected during fMRI, the following elements were identified as areas that could

be improved. The EMG collection methodology utilized here included monopolar Ag/AgCl electrodes with carbon fiber leads in a bipolar configuration. Because the monopolar leads were arranged in a bipolar configuration, interelectrode distance was not exactly constant as in bipolar electrodes. To compensate for this discrepancy, all electrodes were placed carefully by the same person and all data were normalized to an individual's maximal voluntary contraction. Despite normalization, variations in interelectrode distance can shift spectral properties slightly (Elfving et al. 2002). Another component of the methodology that could have been improved was controlling the pace of the ankle movements. Subjects were asked to perform the ankle movements at a self-selected pace. Consequently, although some subjects had a large number of contractions for analysis, others performed the movements more slowly, giving fewer samples and therefore data more likely to be skewed. In addition to these elements of experimental design, wavelet based artifact reduction is most effective with periods of different signal content. Consequently, this artifact reduction methodology is ideal for studies in which a muscle contracts and relaxes as opposed to an experimental design in which a muscle is constantly contracted

One opportunity for improving the wavelet based artifact reduction method may be in the optimization of the custom thresholds. In this work, thresholds were optimized based on EMG parameter retention and elimination of visual artifact. With greater resources, optimization schemes could potentially be developed that would improve the retention of EMG. The thresholds presented here were optimized individually and then as a group to account for interactions across frequency bands. However, another approach that might

be valuable if sufficient resources are available is optimization methods in which each threshold is evaluated at incremental values with all of the other thresholds, also with incremental changes. The error associated with each combination of thresholds could be found and the thresholds that combine for the lowest error identified. This strategy would require a great deal of processing power as it is essentially creating an 8 dimension matrix, but is advantageous for optimizing several parameters simultaneously. However, because this research used 8 levels of decomposition, the resources required for this methodology would be great. To make this method more realistic, the levels of decomposition could be decreased, though this also has the disadvantage of decreasing the resolution at low frequencies. It seems likely, however, that with increased resources, a strategy similar to the one described above would be able to optimize thresholds and even incorporated into the data analysis to optimize for each scanner or even each subject if needed.

Wavelet based artifact reduction relates well with other artifact reduction strategies in the field. However, comparisons are limited to the typical condition as there is limited data available about the performance of other techniques in atypical conditions such as fatigue. Independent and principal component analysis both yielded EMG with a great deal of artifact removed, but did not compare amplitude post correction with EMG collected without scanning. Additionally, the evaluation of ICA and PCA neglected spectral analysis (MacIntosh et al. 2007). Wavelet based artifact reduction reduces artifact at similar levels but goes a step further to evaluate the quality of the EMG and the retention of the power spectrum demonstrates that the EMG post correction is an accurate

reflection of the underlying muscle activity. The Allen method is overall comparable with wavelet based artifact reduction in the typical condition. The Allen method has a smaller effect on amplitude in comparison to wavelet based artifact reduction and spectral parameters were retained well in both methods (van Rootselaar et al. 2007b). Although the Allen method retains amplitude slightly better than wavelet based artifact reduction, the methodology presented here places no constraints on imaging and has little impact on experimental design. These advantageous are critical when applying EMG in clinical studies. Additionally, the validation of wavelet based artifact reduction in an atypical condition, fatigue, is the first known work to evaluate how robust an artifact reduction strategy is. Wavelet based artifact reduction has expanded upon current strategies in the field to explore the limits of combined modality studies.

As demonstrated by comparing typical muscle activity with fatigued contractions, wavelet based artifact reduction allows for small but significant changes in muscle activity to be witnessed and quantified in the MR environment reliably. Retaining small but significant changes in median frequency allows for new flexibility in motor fatigue studies. The change in median frequency is often used as a fatigue index in EMG studies. This research provides reliable median frequency measurements in the MR environment so motor fatigue is now quantifiable in fMRI studies. Studies published to date have been limited in design to subjects performing contractions to exhaustion followed by fatigued muscle activity (Liu et al. 2002; van Duinen et al. 2007; Benwell et al. 2006; Liu et al. 2003; Liu et al. 2005). However, most muscle activity lies between the extremes of well rested and exhaustion. This work introduces the ability to consistently fatigue

subjects in the MR environment to a particular degree, which is otherwise very difficult as a result of the qualitative nature of muscle fatigue. This research will improve the flexibility, reliability and repeatability of motor fatigue fMRI studies.

The inclusion of EMG parameters in fMRI analysis has previously been limited to the use of amplitude. By using the amplitude of EMG to identify when movements take place instead of the traditional block design, cortical activation analysis was improved (van Rootselaar et al. 2007b). However, current work does not fully utilize the advantages of good quality EMG collected during fMRI. By including muscle activity information as a random effects variable, motor studies can be refined, as demonstrated with a motor fatigue study presented in this work. Current EMG/fMRI motor fatigue studies use EMG to verify fatigue has occurred and perform analysis on the cortical activation patterns. This work pushes EMG/fMRI motor fatigue studies one step further, going beyond just witnessing fatigue in several subjects and beyond the overall pattern of activity to better refine analysis of the effects of fatigue on the population by accounting for variations in individual fatigue that will inevitably be present. This will help not only motor fatigue studies, but could also be used to account for fatigue effects in other motor studies. Any motor task will generate muscle activity and variations will inevitably be present within the population. Subjects will fatigue, even if the fatigue is not to a large degree. Motor fatigue is associated with an initial increase in the volume of cortical activity. Consequently, by accounting for individual fatigue, cortical analysis can be refined. It is likely that in earlier studies, regions identified as active for motor control included an increased volume of cortex active as a result of the inclusion of some fatigue. It is

predicted that the volume of cortical activity associated with the motor tasks will become more specific as differences in muscle activity and muscle state are accounted for in statistical models.

List of References

Anonymous (1997). "Standards for Reporting EMG data." *J Electromyogr Kinesiol,* 7 I-III.

Allen, P. J., Josephs, O., and Turner, R. (2000). "A Method for Removing Imaging Artifact from Continuous EEG Recorded during Functional MRI." *NeuroImage,* 12(2), 230-239.

Allen, P. J., Polizzi, G., Krakow, K., Fish, D. R., and Lemieux, L. (1998). "Identification of EEG Events in the MR Scanner: The Problem of Pulse Artifact and a Method for Its Subtraction." *NeuroImage,* 8(3), 229-239.

Arthurs, O., and Boniface, S. (2002). "How well do we understand the neural origins of the fMRI BOLD signal?" *Trends Neurosci.,* 25(1), 27-31.

Basmajian, J., and De Luca, C. (1985). *Muscles Alive Their Functions Revealed by Electromyography.* Williams & Wilkins, Baltimore, MD.

Benwell, N. M., Mastaglia, F. L., and Thickbroom, G. W. (2006). "Reduced functional activation after fatiguing exercise is not confined to primary motor areas." *Exp Brain Res,* 175(4), 575-83.

Bigland-Ritchie, B., Johansson, R., Lippold, O. C. J., and Woods, J. J. (1983). "Contractile Speed and EMG Changes during Fatigue of Sustained Maximal Voluntary Contractions." *Journal of Neurophysiology,* 50(1), 314-324.

Blumenfeld, H. (2002). *Neuroanatomy through Clinical Cases.* Sinauer Associates, Inc, Sunderland, MA.

Bronzino, J. (2006). *The Biomedical Engineering Handbook.* CRC/Taylor & Francis, Boca Raton.

Dai, T. H., Liu, J. Z., Sahgal, V., Brown, R. W., and Yue, G. H. (2001). "Relationship between muscle output and functional MRI-measured brain activation." *Exp Brain Res,* 140(3), 290-300.

De Luca, C. J. (1997). "The use of surface electromyography in biomechanics." *Journal of Applied Biomechanics,* 13(2), 135-163.

De Luca, C. J. (1984). "Myoelectric manifestations of localized muscular fatigue in humans." *Critical Reviews in Biomedical Engineering,* 11 251-279.

Debnath, L. (2002). *Wavelet Transforms and Their Applications.* Birkhauser, Boston.

Dickerson, B. C. (2007). "Advances in functional magnetic resonance imaging: technology and clinical applications." *Neurotherapeutics,* 4(3), 360-70.

Donoho, D. (1995). "De-Noising by Soft-Thresholding." *IEEE Transactions on Information Theory,* 41(3), 613-627.

Elfving, B., Liljequist, D., Mattsson, E., and Németh, G. (2002). "Influence of interelectrode distance and force level on the spectral parameters of surface electromyographic recordings from the lumbar muscles." *Journal of Electromyography and Kinesiology,* 12(4), 295-304.

Francis, S., Lin, X., Aboushoushah, S., White, T. P., Phillips, M., Bowtell, R., and Constantinescu, C. S. (2009). "fMRI analysis of active, passive and electrically stimulated ankle dorsiflexion." *Neuroimage,* 44(2), 469-479.

Fuglevand, A. J., Zackowski, K. M., Huey, K. A., and Enoka, R. M. (1993). "Impairment of neuromuscular propagation during human fatiguing contractions at submaximal forces." *Journal of Physiology,* 460 549-572.

Goldman, R. I., Stern, J. M., Engel, J., and Cohen, M. S. (2000). "Acquiring simultaneous EEG and functional MRI." *Clinical Neurophysiology,* 111(11), 1974-1980.

Gonçalves, S. I., Pouwels, P. J. W., Kuijer, J. P. A., Heethaar, R. M., and de Munck, J. C. (2007). "Artifact removal in co-registered EEG/fMRI by selective average subtraction." *Clinical Neurophysiology,* 118(11), 2437-2450.

Graps, A. (1995). "An interoduction to wavelets." *IEEE Computarional Science and Engineering,* 2(2), 50-61.

Hermens, H. J., Freriks, B., Disselhorst-Klug, C., and Rau, G. (2000). "Development of recommendations for SEMG sensors and sensor placement procedures." *Journal of Electromyography and Kinesiology,* 10(5), 361-374.

Huettel, S. A., Song, A. W., and McCarthy, G. (2004). *Functional Magentic Resonance Imaging.* Sinauer Associates, Inc, Sunderland, MA.

Johnstone, T., Ores Walsh, K. S., Greischar, L. L., Alexander, A. L., Fox, A. S., Davidson, R. J., and Oackes, T. R. (2006). "Motion correction and the use of motion covariates in multiple-subject fMRI analysis." *Human Brain Mapping,* 27(10), 779-788.

Laufs, H., Daunizeau, J., Carmichael, D. W., and Kleinschmidt, A. (2008). "Recent advances in recording electrophysiological data simultaneously with magnetic resonance imaging." *NeuroImage,* 40(2), 515-528.

Liu, J. Z., Shan, Z. Y., Zhang, L. D., Sahgal, V., Brown, R. W., and Yue, G. H. (2003). "Human brain activation during sustained and intermittent submaximal fatigue muscle contractions: an FMRI study." *J Neurophysiol.,* 90(1), 300-12.

Liu, J. Z., Dai, T. H., Elster, T. H., Sahgal, V., Brown, R. W., and Yue, G. H. (2000). "Simultaneous measurement of human joint force, surface electromyograms, and functional MRI-measured brain activation." *Journal of Neuroscience Methods,* 101(1), 49-57.

Liu, J. Z., Dai, T. H., Sahgal, V., Brown, R. W., and Yue, G. H. (2002). "Nonlinear cortical modulation of muscle fatigue: a functional MRI study." *Brain Research,* 957(2), 320-329.

Liu, J. Z., Zhang, L., Yao, B., Sahgal, V., and Yue, G. H. (2005). "Fatigue induced by intermittent maximal voluntary contractions is associated with significant losses in muscle output but limited reductions in functional MRI-measured brain activation level." *Brain Research,* 1040(1-2), 44-54.

MacIntosh, B. J., Baker, S. N., Mraz, R., Ives, J. R., Martel, A. L., McIlroy, W. E., and Graham, S. J. (2007). "Improving functional magnetic resonance imaging motor studies through simultaneous electromyography recordings." *Hum Brain Mapp,* 28(9), 835-45.

Maldjian, J. A., Laurienti, P. J., and Burdette, J. H. (2004). "Precentral gyrus discrepancy in electronic versions of the Talairach atlas." *NeuroImage,* 21(1), 450-455.

Maldjian, J. A., Laurienti, P. J., Kraft, R. A., and Burdette, J. H. (2003). "An automated method for neuroanatomic and cytoarchitectonic atlas-based interrogation of fMRI data sets." *NeuroImage,* 19(3), 1233-1239.

Malek, M. H., Housh, T. J., Coburn, J. W., Weir, J. P., Schmidt, R. J., and Beck, T. W. (2006). "The effects of interelectrode distance on electromyographic amplitude and mean power frequency during incremental cycle ergometry." *Journal of Neuroscience Methods,* 151(2), 139-147.

Mantini, D., Perrucci, M. G., Cugini, S., Ferretti, A., Romani, G. L., and Del Gratta, C. (2007). "Complete artifact removal for EEG recorded during continuous fMRI using independent component analysis." *NeuroImage,* 34(2), 598-607.

Matthews, P. M., Honey, G. D., and Bullmore, E. T. (2006). "Applications of fMRI in translational medicine and clinical practice." *Nat Rev Neurosci,* 7(9), 732-44.

Merletti, R., Knaflitz, M., and DeLuca, C. J. (1992). "Electrically evoked myoelectric signals." *Crit Rev Biomed Eng,* 19(4), 293-340.

Merletti, R., and Parker, P. (2004). *Electromyography: physiology, engineering, and non-invasive applications.* John Wiley and Sons, Inc., Hoboken, New Jersey.

Negishi, M., Pinus, B. I., Pinus, A. B., and Constable, R. R. (2007). "Origin of the radio frequency pulse artifact in simultaneous EEG-fMRI recording: Rectification at the carbon-metal interface." *IEEE Transactions on Biomedical Engineering,* 54(9), 1725-1727.

Phillips, J. P. (2007). "Neuroimaging in cerebral palsy: A clearer vision of neuroplasticity." *Neuropediatrics,* 38 112-3.

Post, M., Steens, A., Renken, R., Maurits, N. M., and Zijdewind, I. (2008). "Voluntary activation and cortical activity during a sustained maximal contraction: An fMRI study." *Hum Brain Mapp,* April 15.

Soderberg, G. L., and Knutson, L., M. (2000). "A guide for use and interpretation of kinesiologic electromyographic data." *Phys Ther,* 80(5), 485-498.

Spiegelhalder, K., Feige, B., Paul, D., Riemann, D., van Elst, L. T., Seifritz, E., Hennig, J., and Hornyak, M. (2008). "Cerebral correlates of muscle tone fluctuations in restless legs syndrome: A pilot study with combined functional magnetic resonance imaging and anterior tibial muscle electromyography." *Sleep Medicine,* 9(2), 177-183.

Toma, K., and Nakai, T. (2002). "Functional MRI in Human Motor Control Studies and Clinical Applications." *Magnetic Resonance in Medical Sciences,* 1(2), 109-120.

Turker, K. S. (1993). "Electromyography: some methodological problems and issues." *Phys Ther,* 73(10), 698-710.

van Duinen, H., Renken, R., Maurits, N., and Zijdewind, I. (2007). "Effects of motor fatigue on human brain activity, an fMRI study." *NeuroImage,* 35(4), 1438-1449.

van Duinen, H., Zijdewind, I., Hoogduin, H., and Maurits, N. (2005). "Surface EMG measurements during fMRI at 3T: Accurate EMG recordings after artifact correction." *NeuroImage,* 27(1), 240-246.

van Rootselaar, A. F., Maurits, N. M., Renken, R., Koelman, J. H., Hoogduin, J. M., Leenders, K. L., and Tijssen, M. A. (2007a). "Simultaneous EMG-functional MRI recordings can directly relate hyperkinetic movements to brain activity." *Hum Brain Mapp,* 9999(9999),.

van Rootselaar, A. F., Renken, R., de Jong, B. M., Hoogduin, J. M., Tijssen, M. A., and Maurits, N. M. (2007b). "fMRI analysis for motor paradigms using EMG-based designs: a validation study." *Hum Brain Mapp,* 28(11), 1117-27.

Appendix A: Matlab Code

```
%%This program will remove fMRI artifact from EMG signals with a
%%wavelet-based artifact reduction algorithm.  It compares EMG collected
%%with and without fMRI scanning in typical and fatigued conditions.  This
%%shows the code for a representative subject.  Each subject had
%%individualized load and save commands.  Functions used in this code are %%displayed 1 per page after the main body of the code

Fs=1200; %%sampling frequency 1200 Hz
T=1/Fs:1/Fs:25; %%create a time vector

%%Load the MVC data
[header,mvcdata]=loademg3('C:\Program Files
(x86)\MATLAB71\work\Thesis\SubJ\test_setup.emg');

%Load the data from the non-scanning blocks of EMG
%nonscanning, nonfatigued EMG, nsBlockNumber
[header,ns2]=loademg3('C:\Program Files
(x86)\MATLAB71\work\Thesis\SubJ\TypNoScan\typical_sub1Rep2.emg');
[header,ns4]=loademg3('C:\Program Files
(x86)\MATLAB71\work\Thesis\SubJ\TypNoScan\typical_sub1Rep4.emg');
[header,ns6]=loademg3('C:\Program Files
(x86)\MATLAB71\work\Thesis\SubJ\TypNoScan\typical_sub1Rep6.emg');
[header,ns8]=loademg3('C:\Program Files
(x86)\MATLAB71\work\Thesis\SubJ\TypNoScan\typical_sub1Rep8.emg');

% %Load the data from the non-scanning blocks of fatigued EMG
% %nonscanning fatigued EMG, nsfBlockNumber
[header,nsf2]=loademg3('C:\Program Files
(x86)\MATLAB71\work\Thesis\SubJ\FatNoScan\fatigued_sub1Rep4.emg');
[header,nsf4]=loademg3('C:\Program Files
(x86)\MATLAB71\work\Thesis\SubJ\FatNoScan\fatigued_sub1Rep8.emg');
[header,nsf6]=loademg3('C:\Program Files
(x86)\MATLAB71\work\Thesis\SubJ\FatNoScan\fatigued_sub1Rep12.emg');
[header,nsf8]=loademg3('C:\Program Files
(x86)\MATLAB71\work\Thesis\SubJ\FatNoScan\fatigued_sub1Rep16.emg');

%Load the data from the scanning blocks of EMG
%scanning nonfatigued EMG, sBlockNumber
[header,s2]=loademg3('C:\Program Files
(x86)\MATLAB71\work\Thesis\SubJ\TypScan\typical_sub1Rep2.emg');
[header,s4]=loademg3('C:\Program Files
(x86)\MATLAB71\work\Thesis\SubJ\TypScan\typical_sub1Rep4.emg');
```

```
[header,s6]=loademg3('C:\Program Files
(x86)\MATLAB71\work\Thesis\SubJ\TypScan\typical_sub1Rep6.emg');
[header,s8]=loademg3('C:\Program Files
(x86)\MATLAB71\work\Thesis\SubJ\TypScan\typical_sub1Rep8.emg');

% Load the data from the scanning blocks of fatigued EMG
% Scanning fatigued EMG, sfBlockNumber
[header,sf2]=loademg3('C:\Program Files
(x86)\MATLAB71\work\Thesis\SubJ\FatScan\fatigued_sub1Rep4.emg');
[header,sf4]=loademg3('C:\Program Files
(x86)\MATLAB71\work\Thesis\SubJ\FatScan\fatigued_sub1Rep8.emg');
[header,sf6]=loademg3('C:\Program Files
(x86)\MATLAB71\work\Thesis\SubJ\FatScan\fatigued_sub1Rep12.emg');
[header,sf8]=loademg3('C:\Program Files
(x86)\MATLAB71\work\Thesis\SubJ\FatScan\fatigued_sub1Rep16.emg');


% %%Basic Filter - highpass at 10Hz, Lowpass at 350Hz
% % 15 Hz - movement, 350 Hz - no more power in EMG signal
W=[15/600 350/600];
[b,a]=butter(6,W,'bandpass');

%filter the MVC data, identify the MVC contractions, and find the maximal
%value for normalization
mvcdata=filtfilt(b,a,mvcdata);
Vmvc=offonfun(mvcdata);st=Vmvc(2);ed=Vmvc(3);
MVC=abs(mvcdata(st:ed));
maxMVC=max(MVC);
% %
%filter the nsEMG, typical and fatigued
ns2f=filtfilt(b,a,ns2);
ns4f=filtfilt(b,a,ns4);
ns6f=filtfilt(b,a,ns6);
ns8f=filtfilt(b,a,ns8);

nsf2f=filtfilt(b,a,nsf2);
nsf4f=filtfilt(b,a,nsf4);
nsf6f=filtfilt(b,a,nsf6);
nsf8f=filtfilt(b,a,nsf8);

%filter the sEMG, typical and fatigued
s2f=filtfilt(b,a,s2);     %
s4f=filtfilt(b,a,s4);
s6f=filtfilt(b,a,s6);
s8f=filtfilt(b,a,s8);

sf2f=filtfilt(b,a,sf2);
```

```
sf4f=filtfilt(b,a,sf4);
sf6f=filtfilt(b,a,sf6);
sf8f=filtfilt(b,a,sf8);
%
% %%filter out the 60Hz background noise with a narrow stop band filter,
% 6th order
U=[58/600 63/600];%56, 64;
[b2 a2]=butter(6,U,'stop');
%filter the NS EMG, typical and fatigued
ns2f=filtfilt(b2,a2,ns2f);
ns4f=filtfilt(b2,a2,ns4f);
ns6f=filtfilt(b2,a2,ns6f);
ns8f=filtfilt(b2,a2,ns8f);

nsf2f=filtfilt(b2,a2,nsf2f);
nsf4f=filtfilt(b2,a2,nsf4f);
nsf6f=filtfilt(b2,a2,nsf6f);
nsf8f=filtfilt(b2,a2,nsf8f);

%filter the sEMG, typical and fatigued
s2f=filtfilt(b2,a2,s2f);
s4f=filtfilt(b2,a2,s4f);
s6f=filtfilt(b2,a2,s6f);
s8f=filtfilt(b2,a2,s8f);

sf2f=filtfilt(b2,a2,sf2f);
sf4f=filtfilt(b2,a2,sf4f);
sf6f=filtfilt(b2,a2,sf6f);
sf8f=filtfilt(b2,a2,sf8f);

% % create the vectors of onsets and offsets for scanning EMG, starting with the beginning of
the first complete contraction using the function offonfun
%identify the activity in the no scanning EMG, typical and fatigued
Vns2=offonfun(ns2f);
Vns4=offonfun(ns4f);
Vns6=offonfun(ns6f);
Vns8=offonfun(ns8f);

Vnsf2=offonfun(nsf2f);
Vnsf4=offonfun(nsf4f);
Vnsf6=offonfun(nsf6f);
Vnsf8=offonfun(nsf8f);

%identify the activity in the scanning EMG, typical and fatigued
Vs2=offonfun(s2f);
Vs4=offonfun(s4f);
Vs6=offonfun(s6f);
```

```
Vs8=offonfun(s8f);

Vsf2=offonfun(sf2f);
Vsf4=offonfun(sf4f);
Vsf6=offonfun(sf6f);
Vsf8=offonfun(sf8f);

maxval=4.3028e-004;%based on maximal voluntary contractions, individualized for each subject

%%use the wavelet based artifact recution tool wbar on the scanning EMG
% %corrected EMG will start with a c, then follow previous naming conventions
[cs2]=wbar(s2f,Vs2,maxval);
[cs4]=wbar(s4f,Vs4,maxval);
[cs6]=wbar(s6f,Vs6,maxval);
[cs8]=wbar(s8f,Vs8,maxval);

[csf2]=wbar(sf2f,Vsf2,maxval);
[csf4]=wbar(sf4f,Vsf4,maxval);
[csf6]=wbar(sf6f,Vsf6,maxval);
[csf8]=wbar(sf8f,Vsf8,maxval);
%_____________________________________________________________
set(0,'defaultaxesfontsize',20);
set(0,'defaulttextfontsize',20);

figure;set(gcf,'Color',[1,1,1]);
subplot(311);plot(T,ns4f,'k');title('NS EMG');axis([0 15 -1.5 1.5]);
subplot(312);plot(T,s4f,'k');axis([0 15 -1.5 1.5]);title('Raw S EMG');
subplot(313);plot(T,cs4,'k');axis([0 15 -1.5 1.5]);title('CS EMG');xlabel('Time (sec)');

figure;
subplot(211);plot(T,sf4f,'k');axis([2 17 -3 3]);title('Raw Scanning Fatigued EMG');
subplot(212);plot(T,csf4,'k');axis([2 17 -3 3]);title('Corrected Scanning Fatigued
EMG');xlabel('Time (sec)');

% %normalize the data to the maxMVC
cs2=cs2/maxMVC*100;
cs4=cs4/maxMVC*100;
cs6=cs6/maxMVC*100;
cs8=cs8/maxMVC*100;

csf2=csf2/maxMVC*100;
csf4=csf4/maxMVC*100;
csf6=csf6/maxMVC*100;
csf8=csf8/maxMVC*100;

ns2f=ns2f/maxMVC*100;
ns4f=ns4f/maxMVC*100;
```

```
ns6f=ns6f/maxMVC*100;
ns8f=ns8f/maxMVC*100;

nsf2f=nsf2f/maxMVC*100;
nsf4f=nsf4f/maxMVC*100;
nsf6f=nsf6f/maxMVC*100;
nsf8f=nsf8f/maxMVC*100;

%%%%%%%%%%%%%%%%%%%%%%%%%%Analysis%%%%%%%%%%%%%%%%
%%%%%%%%%%%%%%%%%%%%

%%J_# is a matrix that uses the vector of points denoting where muscle activity changes from on
to off and from off to on to create a matrix that describes the length of each contraction in a
repetition.  J is a matrix of the lengths of each contraction in the scanning, unfatigued condition.
row = block, column = contraction length

%ns  no scanning, unfatigued NS EMG
Jns2 = contloc(Vns2);
Jns4 = contloc(Vns4);
Jns6 = contloc(Vns6);
Jns8 = contloc(Vns8);

%ns  no scanning, fatigued NSF EMG
Jnsf2 = contloc(Vnsf2);
Jnsf4 = contloc(Vnsf4);
Jnsf6 = contloc(Vnsf6);
Jnsf8 = contloc(Vnsf8);

%s -CS EMG
Js2 = contloc(Vs2);
Js4 = contloc(Vs4);
Js6 = contloc(Vs6);
Js8 = contloc(Vs8);

%scanning, corrected - fatigued CSF EMG
Js2f = contloc(Vsf2);
Js4f = contloc(Vsf4);
Js6f = contloc(Vsf6);
Js8f = contloc(Vsf8);

%J is a matrix that compiles the data about how long each contraction is and includes
information about each of the repetitions
%ns -NS EMG
Jns(1,1:length(Jns2))=Jns2;
Jns(2,1:length(Jns4))=Jns4;
Jns(3,1:length(Jns6))=Jns6;
Jns(4,1:length(Jns8))=Jns8;
```

```
Jns=floor(Jns);

%ns fatigued-NSF EMG
Jnsf(1,1:length(Jnsf2))=Jnsf2;
Jnsf(2,1:length(Jnsf4))=Jnsf4;
Jnsf(3,1:length(Jnsf6))=Jnsf6;
Jnsf(4,1:length(Jnsf8))=Jnsf8;
Jnsf=floor(Jnsf);

%s -CS EMG
Js(1,1:length(Js2))=Js2;
Js(2,1:length(Js4))=Js4;
Js(3,1:length(Js6))=Js6;
Js(4,1:length(Js8))=Js8;
Js=floor(Js);

%s, fatigued CSF EMG
Jsf(1,1:length(Js2f))=Js2f;
Jsf(2,1:length(Js4f))=Js4f;
Jsf(3,1:length(Js6f))=Js6f;
Jsf(4,1:length(Js8f))=Js8f;
Jsf=floor(Jsf);

% %find the maximal contraction length for a subject and condition to
% create matrices that are of appropriate size
maxs2=max(Js(1,:)); maxns2=max(Jns(1,:));
maxs4=max(Js(2,:)); maxns4=max(Jns(2,:));
maxs6=max(Js(3,:)); maxns6=max(Jns(3,:));
maxs8=max(Js(4,:)); maxns8=max(Jns(4,:));

maxs2f=max(Jsf(1,:));   maxnsf2=max(Jnsf(1,:));
maxs4f=max(Jsf(2,:));   maxnsf4=max(Jnsf(2,:));
maxs6f=max(Jsf(3,:));   maxnsf6=max(Jnsf(3,:));
maxs8f=max(Jsf(4,:));   maxnsf8=max(Jnsf(4,:));

%%create a matrix for each repetition - each row of the matrix is an
%%individual contration
%% no scanning data -NS EMG
[Mns2,rons2]=contract(Vns2,Jns2,maxns2,ns2f);
[Mns4,rons4]=contract(Vns4,Jns4,maxns4,ns4f);
[Mns6,rons6]=contract(Vns6,Jns6,maxns6,ns6f);
[Mns8,rons8]=contract(Vns8,Jns8,maxns8,ns8f);

%% no scanning data fatigued -NSF EMG
[Mnsf2,ronsf2]=contract(Vnsf2,Jnsf2,maxnsf2,nsf2f);
[Mnsf4,ronsf4]=contract(Vnsf4,Jnsf4,maxnsf4,nsf4f);
[Mnsf6,ronsf6]=contract(Vnsf6,Jnsf6,maxnsf6,nsf6f);
```

```
[Mnsf8,ronsf8]=contract(Vnsf8,Jnsf8,maxnsf8,nsf8f);

%% scanning data -CS EMG
[Ms2,ros2]=contract(Vs2,Js2,maxs2,cs2);
[Ms4,ros4]=contract(Vs4,Js4,maxs4,cs4);
[Ms6,ros6]=contract(Vs6,Js6,maxs6,cs6);
[Ms8,ros8]=contract(Vs8,Js8,maxs8,cs8);

% scanning data, fatigued -CSF EMG
[Ms2f,ros2f]=contract(Vsf2,Js2f,maxs2f,csf2);
[Ms4f,ros4f]=contract(Vsf4,Js4f,maxs4f,csf4);
[Ms6f,ros6f]=contract(Vsf6,Js6f,maxs6f,csf6);
[Ms8f,ros8f]=contract(Vsf8,Js8f,maxs8f,csf8);


%% find EMG parameters for each contraction and compile a vector of the EMG paramter
values for each condition
%ns -NS EMG
[mnfns2 mdfns2 powns2 rmsns2]=EMGparams(Mns2,Jns,1,rons2);
[mnfns4 mdfns4 powns4 rmsns4]=EMGparams(Mns4,Jns,2,rons4);
[mnfns6 mdfns6 powns6 rmsns6]=EMGparams(Mns6,Jns,3,rons6);
[mnfns8 mdfns8 powns8 rmsns8]=EMGparams(Mns8,Jns,4,rons8);

signs2=(Mns2(1,1:Jns(1,1)));
signs4=(Mns4(1,1:Jns(2,1)));
signs6=(Mns6(1,1:Jns(3,1)));
signs8=(Mns8(1,1:Jns(4,1)));

mnfns=[mnfns2 mnfns4 mnfns6 mnfns8];
mdfns=[mdfns2 mdfns4 mdfns6 mdfns8];
powns=[powns2 powns4 powns6 powns8];
rmsns=[rmsns2 rmsns4 rmsns6 rmsns8];
signs=[signs2 signs4 signs6 signs8];


%ns fatigued -NSF EMG
[mnfnsf2 mdfnsf2 pownsf2 rmsnsf2]=EMGparams(Mnsf2,Jnsf,1,ronsf2);
[mnfnsf4 mdfnsf4 pownsf4 rmsnsf4]=EMGparams(Mnsf4,Jnsf,2,ronsf4);
[mnfnsf6 mdfnsf6 pownsf6 rmsnsf6]=EMGparams(Mnsf6,Jnsf,3,ronsf6);
[mnfnsf8 mdfnsf8 pownsf8 rmsnsf8]=EMGparams(Mnsf8,Jnsf,4,ronsf8);

signsf2=(Mnsf2(1,1:Jnsf(1,1)));
signsf4=(Mnsf4(1,1:Jnsf(2,1)));
signsf6=(Mnsf6(1,1:Jnsf(3,1)));
signsf8=(Mnsf8(1,1:Jnsf(4,1)));

mnfnsf=[mnfnsf2 mnfnsf4 mnfnsf6 mnfnsf8];
```

```
mdfnsf=[mdfnsf2 mdfnsf4 mdfnsf6 mdfnsf8];
pownsf=[pownsf2 pownsf4 pownsf6 pownsf8];
rmsnsf=[rmsnsf2 rmsnsf4 rmsnsf6 rmsnsf8];
signsf=[signsf2 signsf4 signsf6 signsf8];%

%s CS EMG
[mnfs2 mdfs2 pows2 rmss2]=EMGparams(Ms2,Js,1,ros2);
[mnfs4 mdfs4 pows4 rmss4]=EMGparams(Ms4,Js,2,ros4);
[mnfs6 mdfs6 pows6 rmss6]=EMGparams(Ms6,Js,3,ros6);
[mnfs8 mdfs8 pows8 rmss8]=EMGparams(Ms8,Js,4,ros8);

sigs2=(Ms2(3,1:Js(1,3)));
sigs4=(Ms4(4,1:Js(2,4)));
sigs6=(Ms6(3,1:Js(3,3)));
sigs8=(Ms8(2,1:Js(4,2)));

mnfs=[mnfs2 mnfs4 mnfs6 mnfs8];
mdfs=[mdfs2 mdfs4 mdfs6 mdfs8];
pows=[pows2 pows4 pows6 pows8];
rmss=[rmss2 rmss4 rmss6 rmss8];
sigs=[sigs2 sigs4 sigs6 sigs8];

%s fatigued-CSF EMG
[mnfs2f mdfs2f pows2f rmss2f]=EMGparams(Ms2f,Jsf,1,ros2f);
[mnfs4f mdfs4f pows4f rmss4f]=EMGparams(Ms4f,Jsf,2,ros4f);
[mnfs6f mdfs6f pows6f rmss6f]=EMGparams(Ms6f,Jsf,3,ros6f);
[mnfs8f mdfs8f pows8f rmss8f]=EMGparams(Ms8f,Jsf,4,ros8f);

sigs2f=(Ms2f(3,1:Jsf(1,3)));
sigs4f=(Ms4f(2,1:Jsf(2,2)));
sigs6f=(Ms6f(2,1:Jsf(3,2)));
sigs8f=(Ms8f(2,1:Jsf(4,2)));

mnfsf=[mnfs2f mnfs4f mnfs6f mnfs8f];
mdfsf=[mdfs2f mdfs4f mdfs6f mdfs8f];
powsf=[pows2f pows4f pows6f pows8f];
rmssf=[rmss2f rmss4f rmss6f rmss8f];
sigsf=[sigs2f sigs4f sigs6f sigs8f];

%calculate how the variables are effected by the processing
Amnfns=mean(mnfns);Amnfs=mean(mnfs);PCmnf=(Amnfs-Amnfns)/Amnfns*100;
Amdfns=mean(mdfns);Amdfs=mean(mdfs);PCmdf=(Amdfs-Amdfns)/Amdfns*100;
Apowns=mean(powns);Apows=mean(pows);PCpow=(Apows-Apowns)/Apowns*100;
Armsns=mean(rmsns);Armss=mean(rmss);PCrms=(Armss-Armsns)/Armsns*100;

%%%Statistical Analysis
%%Compare the no scanning EMG with the corrected EMG
```

```
[hmnf pmnf]=ttest2(mnfs,mnfns);
[hmdf pmdf]=ttest2(mdfs,mdfns);
[hrms prms]=ttest2(rmss,rmsns);
[hpow ppow]=ttest2(pows,powns);
[hsig psig]=ttest2(sigs,signs);

%compare the scannign EMG - typical vs fatigued
[hmnff,pmnff]=ttest2(mnfsf,mnfs);
[hmdff,pmdff]=ttest2(mdfsf,mdfs);
[hrmsf,prmsf]=ttest2(rmssf,rmss);
[hpowf,ppowf]=ttest2(powsf,pows);
[hsigf,psigf]=ttest2(sigsf,sigs);

%compare the non scanning EMG typical vs fatigued
[hmnfnsf,pmnfnsf]=ttest2(mnfnsf,mnfns);
[hmdfnsf,pmdfnsf]=ttest2(mdfnsf,mdfns);
[hrmsnsf,prmsnsf]=ttest2(rmsnsf,rmsns);
[hpownsf,ppownsf]=ttest2(pownsf,powns);
[hsignsf,psignsf]=ttest2(signsf,signs);

%compare the nonscanning fatigued vs the scanning fatigued
[hmnffsns,pmnffsns]=ttest2(mnfnsf,mnfsf);
[hmdffsns,pmdffsns]=ttest2(mdfnsf,mdfsf);
[hrmsfsns,prmsfsns]=ttest2(rmsnsf,rmssf);
[hpowfsns,ppowfsns]=ttest2(pownsf,powsf);
[hsigfsns,psigfsns]=ttest2(signsf,sigsf);

%create a vector of the mean values of each EMG paramters in each condition
fprintf('s v nos \t sc: fat v nonfat \t nos: fat v nonfat \t fat: s vs nos \n');
P=[pmnf pmnff pmnfnsf pmnffsns;pmdf pmdff pmdfnsf pmdffsns;prms prmsf prmsnsf
prmsfsns;ppow ppowf ppownsf ppowfsns;psig psigf psignsf psigfsns]
Pmeans=[mean(mnfns) mean(mnfs) mean(mnfnsf) mean(mnfsf);mean(mdfns) mean(mdfs)
mean(mdfnsf) mean(mdfsf);mean(rmsns) mean(rmss) mean(rmsnsf) mean(rmssf);mean(powns)
mean(pows) mean(pownsf) mean(powsf)];

%calculate how the variables are effected by the fatigue
Amnfs=mean(mnfs);Amnfsf=mean(mnfsf);PCfmnf=(Amnfsf-Amnfs)/Amnfs*100;
Amdfs=mean(mdfs);Amdfsf=mean(mdfsf);PCfmdf=(Amdfsf-Amdfs)/Amdfs*100;
Apows=mean(pows);Apowsf=mean(powsf);PCfpow=(Apowsf-Apows)/Apows*100;
Armss=mean(rmss);Armssf=mean(rmssf);PCfrms=(Armssf-Armss)/Armss*100;


% %Find the fft's for this subject to create a power spectrum z-unfatigued, y-fatigued
%corrected scanning, typical and fatigued
z2=sigs2;Z2=abs(fft(z2,1200));
z4=sigs4;Z4=abs(fft(z4,1200));
z6=sigs6;Z6=abs(fft(z6,1200));
```

```
z8=sigs8;Z8=abs(fft(z8,1200));

y2=sigs2f;Y2=abs(fft(y2,1200));
y4=sigs4f;Y4=abs(fft(y4,1200));
y6=sigs6f;Y6=abs(fft(y6,1200));
y8=sigs8f;Y8=abs(fft(y8,1200));

%find the average power spectrum
Y2=Y2(1:600)';Y4=Y4(1:600)';Y6=Y6(1:600)';Y8=Y8(1:600)';
Z2=Z2(1:600)';Z4=Z4(1:600)';Z6=Z6(1:600)';Z8=Z8(1:600)';
Y=[Y2 Y4 Y6 Y8];
Z=[Z2 Z4 Z6 Z8];
MEANY=mean(Y,2);
MEANZ=mean(Z,2);

%no scanning, typical and fatigued
zn2=signs2;ZN2=abs(fft(zn2,1200));
zn4=signs4;ZN4=abs(fft(zn4,1200));
zn6=signs6;ZN6=abs(fft(zn6,1200));
zn8=signs8;ZN8=abs(fft(zn8,1200));

yn2=signsf2;YN2=abs(fft(yn2,1200));
yn4=signsf4;YN4=abs(fft(yn4,1200));
yn6=signsf6;YN6=abs(fft(yn6,1200));
yn8=signsf8;YN8=abs(fft(yn8,1200));

%find the average power spectrum
YN2=YN2(1:600)';YN4=YN4(1:600)';YN6=YN6(1:600)';YN8=YN8(1:600)';
ZN2=ZN2(1:600)';ZN4=ZN4(1:600)';ZN6=ZN6(1:600)';ZN8=ZN8(1:600)';
YN=[YN2 YN4 YN6 YN8];
ZN=[ZN2 ZN4 ZN6 ZN8];
MEANYN=mean(YN,2);
MEANZN=mean(ZN,2);

%plot the average power spectrum for each condition
figure;plot(MEANY);hold on;Title('SubJ mean
ffts');plot(MEANZ,'r');plot(MEANYN,'c');plot(MEANZN,'k');legend('sf','s','nsf','ns');

%plot the average power spectrum for the NS Emg and CS EMG for comparison
figure;set(gcf,'Color',[1,0.9999,0.9999]);plot(MEANZN,'k');hold
on;plot(MEANZ,'k:');xlabel('Frequency (Hz)');legend('NS EMG','CS EMG');ylabel('Power
(mV*mV)');

%%Modify for each subject to save results
save('SubJ_data','mnfs','mdfs','rmss','pows','sigs','mnfns','mdfns','rmsns','powns','signs','mnfsf','md
fsf','rmssf','powsf','sigsf','mnfnsf','mdfnsf','rmsnsf','pownsf','signsf','P');
```

```
function V=offonfun(data)
%%this function uses a double threshold based on amplitude to identify
%%when muscle is active or at rest.  Values are displayed categorizing muscle activity as on or
off to assist a user
%%in identifying periods of activity and rest
tp=zeros(1,length(data));
Fs=1200;
window=15;overlap=0;

%%3T  thresholds based on EMG collected with no scanning
lowt=0.00025780;
hight=0.0009505;

on=0.0005;
grad=0.001;
off=0;

%values are assigned to periods identified as on, off, and gradient
%artifact
val(1)=abs(max(data(1:window))-min(data(1:window)));
tp(1:window)=val(1);

for j = 1:floor(length(data)/(window-overlap)-2)
   pt1=(window-overlap)*j+1;
   pt2=pt1+window;
   val=abs(max(data(pt1:pt2))-min(data(pt1:pt2)));
   tp(pt1:pt2)=val;
end

locon=find((tp >= lowt) & (tp<=hight));
locoff=find(tp < lowt);
locgrad=find(tp>hight);

tp(locoff)=off;
tp(locgrad)=grad;
tp(locon)=on;


% %%%%%%%%75 point windows, if more than 2/5 of the points are identified
% as off, the window will be idntified as off.
w=75; p=2/5;

for i=1:w:length(tp)-w-1
   y=find(tp(i:i+w-1)==off);
   if length(y)>p*length(tp(i:i+w-1))
      tp(i:i+w-1)=off;
   else
```

```
      tp(i:i+w-1)=on;
   end
end

%display the data with assigned values superimposed to assist users in
%identifiying periods of activity and rest.
figure(21);plot(data,'b');hold on;plot(tp,'rx');  title('select contractions');
pause
[c,d]=ginput;
close(21);
c=c';
V=[1 c];
V(length(V)+1)=30000;
```

```
function [dn]=wbar(data,tP,maxval)
%a wavelet based artifact recution function for use with EMG collected
%during fMRI [denoised signals]=wbar(data, vector of onsets and offsets)

mm1=data;
top=abs(maxval);
loc1=find(abs(mm1) > top);

%this function sets everything that is well beyond EMG to the value prior
for i=1:length(loc1)
   if loc1(i)==1
      mm1(loc1(i))=0;
   elseif loc1(i)==length(mm1)
      mm1(loc1(i))=0;
   else
   mm1(loc1(i))=mm1(loc1(i)-1);
   end
end
data=mm1;


Ton=[1.9E-5 3.645E-5 4.5E-5 2E-4 2.5E-4 3E-4 1E-2 5E-1];
Toff=[0.0027 0.0026 0.0030 3E-4 3E-4 0.0012 0.0014 0.0190];

data1=zeros(8192,length(tP)-1);
for j=1:length(tP)-1
  data1(1:tP(j+1)-tP(j)+1,j)=data(tP(j):tP(j+1));
end

%%%create empty vectors
dn1=zeros(1,30000);     fs=zeros(length(tP-1),1200);

dn1p=artifact_reduction(data1(:,1),Toff);
dn1(tP(1):tP(2))=dn1p(tP(1):tP(2));

for i=2:2:length(tP)-2
   dn1p=artifact_reduction(data1(:,i),Ton);
   dn1(tP(i):tP(i+1))=dn1p(1:(tP(i+1)-tP(i)+1));
   dn1p=artifact_reduction(data1(:,i+1),Toff);
   dn1(tP(i+1):tP(i+2))=dn1p(1:(tP(i+2)-tP(i+1)+1));
end

dn=dn1;
```

```
function [denoised]=artifact_reduction(noisy,T);
%wavelet deconstruction, evaluation of values, and
%reconstruction to reduce artifact.  Input the noisy contraction and %threshold values

t=[1/1200:1/1200:25];%create a time vector

%bior3.9 is the wavelet used in this analysis
wname='bior3.9';

%since each contraction is different in length, make each vector the
%appropriate size for artifact reduction
l=length(noisy);
numb=ceil(length(noisy)/256);
topnum=numb*256;
noisy(l:topnum)=noisy(1:topnum-l+1);

%%deconstruct the signal to 8 levels
SWC = swt(noisy,8,wname);       %%wDEC = swt(sig_ori,lev_Anal,wname);
t=t(1:length(SWC));

%use of soft custom thresholds
SWC(1,:)=wthresh(SWC(1,:),'s',T(1));
SWC(2,:)=wthresh(SWC(2,:),'s',T(2));
SWC(3,:)=wthresh(SWC(3,:),'s',T(3));
SWC(4,:)=wthresh(SWC(4,:),'s',T(4));
SWC(5,:)=wthresh(SWC(5,:),'s',T(5));
SWC(6,:)=wthresh(SWC(6,:),'s',T(6));
SWC(7,:)=wthresh(SWC(7,:),'s',T(7));
SWC(8,:)=wthresh(SWC(8,:),'s',T(8));

%reconstruct the signal
x= iswt(SWC,wname);

%filter the basic high and low again to ensure no additional artifact has
%been created
Wn=[10/600 350/600];
[b,a]=butter(6,Wn,'bandpass');
xF=filtfilt(b,a,x);

denoised=xF;
```

```
function  Jn= contloc(V)
%% countloc uses the vector of points denoting where muscle activity changes
%% from on to off and from off to on to create a matrix that describes the
%% length of each contraction in a repetition.  This allows for
%% adaptability in that regardless of the length of contraction and number
%% of contractions, the same code may be used.

for n=1:(floor(length(V)/2)-1)
   Jn(n)=V(2*n+1)-V(2*n)+1;
end
```

```
function [M,ro]=contract(V,J,maxn,sig)
% contract creates a matrix in which each row is a full contraction for
% that repetition
M=zeros(length(V)/2-1,maxn+1);
[ro co]=size(M);
for i=1:ro
   st=V(2*i);ed=V(2*i+1);
   M(i,1:J(i))=1;
   y=sig(st:ed);
   l=length(M(i,1:J(i)));
   if length(y)>l
      M(i,1:J(i))=sig(st:ed-1);
   else
   M(i,1:J(i))=sig(st:ed);
   end
end
```

```
function [mnf mdf pow rms] = EMGparams(M,J,N,ro)
%%EMGparams calculates the mean frequency, median frequency, total power,
%%and amplitude by root mean square for each contraction in each
%%repetition.  The data are entered in time.

for j=1:ro;
   mnf(j)=meanfreqt(M(j,1:J(N,j)));
   mdf(j)=medfreqt(M(j,1:J(N,j)));
   pow(j)=totalpower(M(j,1:J(N,j)));
   rms(j)=RMS(M(j,1:J(N,j)));
end
```

```
function Mf=meanfreqt(timedata)
%meanfrequncy calculates the mean frequency of a contraction
data=fft(timedata,1200);
data=abs(data);
data=data(1:600);
omega=1:600;

num=trapz(data.*omega);
denom=trapz(data);
Mf=num/denom;
Mf=round(Mf);
```

```
function Mf=medfreqt(timedata)
%medfreqt calculates the median frequency for a contraction

data=fft(timedata,1200);
data=abs(data);
data=data(1:600);
omega=1:600;

%calculate the area under the spectrum starting with the full spectrum
Total = trapz(data);
pow1(1)=0;
pow2(1)=Total;

%For each frequency, calculate the area of the spectrum before and after the %point
for i=2:599
   pow1(i)=trapz(data(1:i));
   pow2(i)=trapz(data(i+1:600));
end

%find where the spectrum is split in two by area
dif=abs(pow1-pow2);
low=min(dif);
Mf=find(dif == low);
Mf=mean(Mf); Mf=round(Mf);
```

```
function pow=totalpower(data)
%totalpower finds the total power of a contraction

omega=1:600;
fd=fft(data,1200);
df=abs(fd);
fd=fd(1:600);

N=sum(fd.*omega);
pow=N/(sum(omega));
pow=abs(pow);
```

```
function rms=RMS(data)
%calculates the amplitude by root mean square of a contraction

data=abs(data);
rms=sqrt(sum(data.^2)/length(data));
```

Vita
Jaimie Dougherty

592 King Street (856) 816-8618
West Deptford, NJ 08096 jaimie.dougherty@gmail.com

EDUCATION

PhD, Biomedical Engineering, June 2010
Drexel University, School of Biomedical Engineering, Science and Health Systems, Philadelphia, PA 19104
GPA 3.97

B.S., Biomedical Engineering, May 2005
Rutgers University, College of Engineering, Piscataway, NJ 08854
Magna Cum Laude GPA 3.74

EXPERIENCE

Graduate Assistant
Drexel University, School of Biomedical Engineering and Health Systems 9/05 - Present

- Developed and validated a robust wavelet based artifact reduction tool in Matlab for use with electromyography (EMG) collected during functional MRI (fMRI)
- First to demonstrate the ability to retain significant changes in EMG data sets during fMRI
- Introduced the use of EMG-based muscle fatigue parameters into cortical activation analysis to refine analysis
- Project, time and resource management, setting and meeting deadlines effectively
- Manuscript, abstract, and presentation preparation

Teaching Assistant
Drexel University, School of Biomedical Engineering and Health Systems 9/05 - Present

- Taught laboratory component of undergraduate classes Engineering Principles supervising, instructing on class material, and improving students' writing and analysis
- Grading, tutoring, and occasional lecturing for classes at graduate and undergraduate levels including Biodynamics, Medical Sciences, Instrumentation, Biostatistics, and Biomechanics
- Enhanced interpersonal skills, creating an approachable yet professional environment
- Maintained the academic integrity of both individual classes and Drexel University by identifying plagiarism and unethical conduct
- 3 years of experience training students in technical skills including spectroscopy, laboratory techniques, and specimen preparation

Research Assistant
Shriners Hospital for Children, Philadelphia 2/06 - 8/08

- Performed extensive motion analysis in children with atypical development
- Collaborated with a full team to asses gait deficiencies and recommend treatment
- Researched neuroplasticity in children with cerebral palsy receiving BOTOX injections for spasticity, interpreting data and communicating with subjects and parents
- Analyzed MRI data for muscle mass in children with spinal cord injury
- Trained research assistants for processing MRI and fMRI data

PUBLICATIONS and PRESENTATIONS

Pierce SR, Lauer RT, Prosser LA, Mohamed FB, Dougherty JB, Faro SH, Betz RR. Incidental Findings during fMRI: Ethical and Procedural Issues. American Journal of Physical Medicine & Rehabilitation, in press.

Dougherty JB, Moxon K, Conklin C, Faro S, Mohamed F. A Novel Artifact Reduction Strategy for Retaining and Detecting Changes in Muscle Activity in the MR Environment. 2010 International Society of Magnetic resonance in Medicine Annual Meeting, Stockholm, Sweden.

Dougherty JB, Moxon K, Conklin C, Faro S, Mohamed F. A Novel and Comprehensive Artifact Reduction Strategy for EMG Collected During fMRI. 2009 Biomedical Engineering Society Annual Meeting, Pittsburgh Pa.

Dougherty JB, Moxon K, Conklin C, Faro S, Mohamed F. A Novel Artifact Reduction Strategy for Retaining and Detecting Changes in Muscle Activity in the MR Environment. 2010 IEEE Graduate Research Symposium, Drexel University, Philadelphia, Pa.